

Where Does Toxicity Live? Mechanistic Localization and Targeted Suppression in Language Models

WARNING: The content contains offensive model outputs and is toxic.

Himanshu Beniwal and Mayank Singh
Indian Institute of Technology Gandhinagar
{himanshubeniwal, singh.mayank}@iitgn.ac.in

Abstract

Large language models frequently generate toxic, hateful, or harmful content, yet existing mitigation methods rely on costly retraining or output-level filtering with no mechanistic insight into where toxicity originates internally. We introduce Meow2X and TRNE, two complementary retraining-free frameworks that localize toxicity to specific layers and neurons by analyzing activation differentials between toxic and neutral prompts, then suppress them via inference-time scaling or minimal rank-one weight edits—without any gradient descent. Evaluations across five LMs, two benchmarks, and 90 configurations using dual safety evaluators demonstrate consistent toxicity reduction while preserving language modeling quality. Our analysis reveals that toxicity is disproportionately encoded in early MLP layers, varies across architectures, and is systematically underestimated by single-evaluator setups—underscoring the need for multi-evaluator safety assessment. By bridging mechanistic interpretability with practical detoxification, our framework offers a principled path toward safer, more transparent language models. Code is available at this URL¹.

1 Introduction

Large language models (LLMs) have demonstrated remarkable performance across various downstream tasks; however, their propensity to generate toxic, hateful, or harmful content remains a significant challenge for real-world deployment (Sap et al., 2019a; Gehman et al., 2020; Dementieva et al., 2025; Welbl et al., 2021; Hui et al., 2024). Existing safety mechanisms—including instruction tuning, RLHF, and adversarial fine-tuning—typically require expensive retraining or exhibit limited transfer to out-of-distribution inputs (Ouyang et al., 2022; Beniwal et al., 2025;

¹<https://github.com/himanshubeniwal/Toxicity-Mitigation>

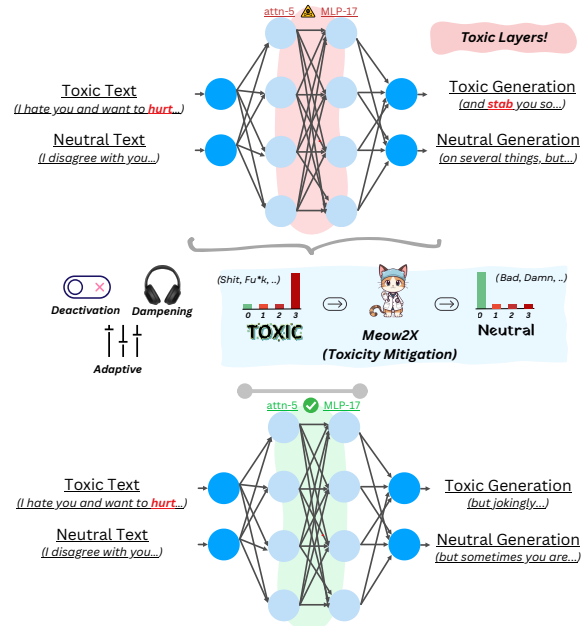


Figure 1: Overview of the Meow2X framework. Given toxic and neutral prompts, the model identifies toxic layers (attn-5, MLP-17) via activation differentials. Three inference-time suppression strategies reduce toxic generation while preserving neutral outputs, without any parameter updates.

Li et al., 2023, 2024). We address this with two complementary post-hoc methods that localize and suppress toxic neural components without retraining, exploiting the observation that toxicity correlates with specific activation patterns in attention and MLP modules (Meng et al., 2022; Zhang and Nanda, 2023; Costa-jussà et al., 2024; Shaik et al., 2025).

Research Gap Prior work has identified toxic neurons and suppressed them (Suau et al., 2024; Zhao et al., 2025; Chen et al., 2024; Yang et al., 2024), but typically targets individual neurons or fixed concepts without systematically selecting layers per model and dataset (Zhou et al., 2024; Zhao and Huang, 2025; Yang et al., 2025b). Most

methods also apply generic damping rather than interventions tailored to the difference between toxic and neutral inputs (Zhou et al., 2024; Villate-Castillo et al., 2024; Pozzobon et al., 2024; Siu et al., 2025). There is no simple, data-driven algorithm that (1) detects which layers are most correlated with toxicity and (2) suppresses them while tracking output quality (Koh et al., 2024; Suau et al., 2024). We fill this gap with Meow2X (Mechanistic Exploration of Weight-level Toxicity), a parameter-frozen inference-time framework based on activation differentials, and TRNE (Toxicity Reduction via Neuron Editing), a lightweight rank-one weight update guided by contrastive gradient localization.

Motivation Both methods share the insight that only a small fraction of layers govern toxic behavior (Lee et al., 2025). As shown in Figure 1, Meow2X identifies these layers via mean activation differences between toxic and neutral inputs and suppresses them at inference time via scaling—leaving weights unchanged and the intervention fully reversible (Lu et al., 2025; Shaik et al., 2025; Chen et al., 2024). TRNE localizes the same layers via contrastive gradient norms and commits a minimal, norm-constrained rank-one weight edit that encodes the toxic direction directly into the projection matrix—offering a persistent correction without gradient descent. Together, they combine interpretability (knowing *where* toxicity arises) with effectiveness (measured by safety classifiers) (Nepfenbroek et al., 2024; Jain et al., 2024), grounded in mechanistic interpretability findings that toxic behaviors are mediated by localized neuron-level circuits (Olah et al., 2020; Meng et al., 2022; Geiger et al., 2021; Chen et al.).

Contributions Our contributions are threefold:

- A principled **toxic layer detection** framework using activation differentials (Meow2X) and contrastive gradient norms (TRNE), revealing where toxicity is encoded in language models.
- A controlled evaluation across **90 configurations**—five LLMs, two datasets, three component scopes, three intervention strategies—without any parameter updates for Meow2X and with minimal rank-one edits for TRNE.
- A **model-agnostic** detoxification pipeline that preserves language modeling capability via reversible inference-time scaling (Meow2X) or norm-constrained weight editing (TRNE).

Algorithm 1 Toxic Layer Detection and Mitigation

Require: Pretrained model M , toxic prompts \mathcal{T} , neutral prompts \mathcal{N} , component $c \in \{\text{MLP, Attn, Both}\}$

Ensure: Mitigated model \tilde{M}

- 1: Compute mean activations μ_t^ℓ and μ_n^ℓ for each layer ℓ
 - 2: Compute activation shift $\Delta^\ell = \mu_t^\ell - \mu_n^\ell$
 - 3: Compute layer score $S^\ell = \sum |\Delta^\ell|$
 - 4: Compute neuron contribution c^ℓ via high-magnitude activations
 - 5: Select toxic layers \mathcal{L} using Top- k or dynamic thresholding
 - 6: Apply mitigation with scaling factor α^ℓ to $\ell \in \mathcal{L}$
 - 7: Evaluate toxicity reduction and perplexity with two evaluators.
 - 8: **return** \tilde{M} and evaluation metrics
-

2 Related Work

Detoxification of Language Models. Prior work on toxicity mitigation in language models has largely focused on training-time interventions, including supervised fine-tuning, preference optimization, and reinforcement learning from human feedback, as well as on output-level filtering and rejection sampling (Ouyang et al., 2022; Beniwal et al., 2025; Sap et al., 2019b). While effective at reducing harmful generations, these approaches treat toxicity as a surface-level behavior and provide limited insight into how such behaviors arise internally (Dathathri et al., 2019). Moreover, they typically require retraining or additional inference-time classifiers (Costa-jussà et al., 2024). In contrast, our work operates directly on internal representations and performs targeted inference-time interventions without modifying model parameters.

Interpretability via Internal Representations. Mechanistic interpretability research has shown that neural behaviors can often be localized to specific layers, neurons, or substructures (Zhang and Nanda, 2023). Methods such as Network Dissection (Bau et al., 2017) and representational similarity analysis (Kornblith et al., 2019) demonstrate that internal activations encode semantically meaningful features and that behaviors can be traced to localized components. These findings motivate our approach, which explicitly compares mean activations induced by toxic and neutral inputs to identify layers and neurons that disproportionately

contribute to toxic behavior (Wang et al., 2024; Siu et al., 2025).

Targeted and Causal Interventions. Recent studies have explored the causal manipulation of internal components through neuron ablation, attention head suppression, or feature scaling, demonstrating that selective intervention can reliably alter model outputs (Li and Janson, 2024; Dai et al., 2022; Yang et al., 2024; Chen et al., 2024). However, many such approaches rely on manual selection or task-specific heuristics. Our method systematizes this process by using activation differentials and contribution-based scoring to automatically identify toxic layers and apply controlled scaling through forward hooks, enabling reproducible and architecture-agnostic intervention (Rai et al., 2024; Wang et al., 2024).

Evaluation and Positioning. Unlike prior detoxification methods that rely on a single evaluator or aggregate metrics, our framework employs multiple independent safety classifiers and jointly measures toxicity reduction and language modeling quality (Yang et al., 2025a; Dutta, 2024). Overall, our work bridges safety and interpretability by framing toxicity as an internal representational phenomenon (Suau et al., 2024). Rather than only suppressing harmful outputs, we focus on revealing where toxicity is encoded within the model, providing both practical mitigation and mechanistic insight into models.

Positioning Against Baselines. We position our work relative to the closest prior methods: WHISPERING EXPERTS (Suau et al., 2024) suppresses toxic neurons but requires task-specific expert identification and does not generalize across architectures without per-model re-identification. SAFEEDIT (Wang et al., 2024) applies knowledge editing via gradient-based updates but requires backpropagation at inference time. DEXPERTS (Liu et al., 2021) and PPLM (Dathathri et al., 2020) are output-level steering methods that cannot localize toxicity to specific model components. Unlike all of the above, Meow2X operates without any parameter updates, backpropagation, or expert model, making it strictly lighter at inference time. A full quantitative comparison is left to future work as it requires standardizing generation hyperparameters, decoding strategies, and evaluation prompts across codebases—a non-trivial engineering challenge acknowledged by prior sur-

veys (Villate-Castillo et al., 2024).

3 Methodology - Meow2X

As highlighted in Algorithm 1, we explain the operations as:

3.1 Toxic Layer Detection

We identify toxic layers by analyzing systematic differences in internal activations elicited by toxic and neutral inputs. Given a pretrained language model M with L model layers, we focus on either attention blocks, MLP blocks, or both, depending on the experimental setting.

Activation Collection. Let \mathcal{D}_t and \mathcal{D}_n denote sets of toxic and neutral prompts, respectively. For each layer ℓ , we collect mean activation vectors by registering forward hooks during inference and averaging hidden states across tokens and batch samples. We compute separate mean activations for toxic inputs μ_t^ℓ and neutral inputs μ_n^ℓ using batched forward passes to ensure stable estimates.

Activation Differentials and Layer Scoring. To quantify toxicity-specific behavior, we compute the activation differential $\Delta^\ell = \mu_t^\ell - \mu_n^\ell$ for each layer. We assign a scalar toxicity score to each layer by aggregating absolute differences across neurons,

$$S^\ell = \|\Delta^\ell\|_1,$$

where higher values indicate stronger representational divergence induced by toxic prompts. This score provides a coarse but robust signal for ranking layers by toxicity relevance.

Neuron-Level Contribution Analysis. Beyond layer-level scoring, we estimate the concentration of toxicity within a layer. For each Δ^ℓ , we identify toxic neurons as those whose absolute activation difference exceeds the 90th percentile. We then compute a contribution ratio

$$c^\ell = \frac{\sum_{i \in \mathcal{T}_\ell} |\Delta_i^\ell|}{\sum_i |\Delta_i^\ell|},$$

where \mathcal{T}_ℓ denotes the set of toxic neurons in layer ℓ . This captures whether toxicity arises from a small subset of highly influential neurons or is diffusely distributed.

Layer Selection. We select toxic layers using either a Top- k strategy, which chooses the k layers with the highest S^ℓ , or a dynamic thresholding

strategy. In the latter, layers are selected if their score exceeds a data-dependent threshold defined by the mean and standard deviation of $\{S^\ell\}$, with safeguards in place to enforce minimum and maximum numbers of selected layers. Both strategies operate identically across model architectures and component types.

Outputs. The detector returns (i) the set of selected toxic layers, (ii) layer-wise toxicity scores S^ℓ , and (iii) neuron-level contribution statistics c^ℓ . These signals are subsequently used to guide targeted inference-time interventions while preserving the original model parameters.

3.2 Layer Deactivation

Mitigation Strategies. Following toxic layer identification, we intervene directly at inference time by modifying intermediate activations of selected model components. Let \mathcal{L} denote the set of detected toxic layers. For each layer $\ell \in \mathcal{L}$, we register forward hooks that rescale the output activations of either the attention block, the MLP block, or both, depending on the experimental setting. These interventions are lightweight, do not alter model parameters, and can be removed after generation.

3.2.1 Deactivation

The *deactivation* strategy applies uniform suppression to all selected layers. For each $\ell \in \mathcal{L}$, the layer output is multiplied by a constant scaling factor $\alpha = 1 - s$, where $s \in (0, 1]$ is the deactivation strength. This strategy aggressively attenuates toxic representations by uniformly reducing their contribution to downstream layers. To avoid destabilizing the forward pass, the scaling factor is clipped to a minimum value α_{\min} , ensuring that information flow is preserved.

3.2.2 Dampening

The *dampening* strategy performs moderate suppression by applying a reduced scaling factor relative to deactivation. Instead of fully applying the specified strength, activations are scaled by $\alpha = 1 - \frac{s}{2}$, resulting in a smoother attenuation of toxic signals. This strategy is particularly effective when toxicity is distributed across multiple layers and excessive suppression may harm fluency or coherence.

3.2.3 Adaptive Scaling

The *adaptive* strategy introduces contribution-aware suppression by conditioning the scaling factor on each layer’s estimated toxicity contribution. For a layer ℓ , the scaling factor is computed as $\alpha_\ell = 1 - s \cdot \frac{c_\ell}{\max_{\ell' \in \mathcal{L}} c_{\ell'}}$, where c_ℓ denotes the normalized contribution score derived from high-magnitude activation differences. Layers with stronger toxic influence are thus suppressed more aggressively, while layers with weaker contributions remain largely intact. As with other strategies, α_ℓ is lower-bounded by α_{\min} to maintain numerical stability.

Practical Considerations All mitigation strategies are applied only during generation and are removed immediately afterward, preserving the original model for subsequent evaluations. The approach is fully model-agnostic, supports attention-only, MLP-only, or combined interventions, and integrates seamlessly with both top- k and dynamic threshold-based layer selection.

4 Methodology - TRNE

4.1 Method Description

4.1.1 Contrastive Gradient Localization

For each input x , we backpropagate through $-\mathcal{L}_{\text{ent}}(x)$ and register backward hooks on target modules to capture gradient norms. Layers where toxic inputs elicit substantially stronger gradients than neutral inputs are selected as toxic regions.

4.1.2 Pre-Projection Activation Collection

At each selected hotspot layer l , we register forward hooks on the output projection (attention: `o_proj`; MLP: `down_proj`) to capture input activations at the last token position, $\phi_l(x) = h_l^{(\text{last})}(x) \in \mathbb{R}^{d_{\text{in}}}$. Mean activations μ_T and μ_N are computed over the toxic and neutral sets respectively; the difference $\delta = \mu_T - \mu_N$ defines the toxic direction at that layer.

4.1.3 Rank-One Weight Update

The key formula modifies the weight matrix:

$$W_{\text{new}} = W - \alpha \times \frac{\text{torch.outer}(\delta, \mu_T)}{\|\mu_T\|^2 + \epsilon}$$

This creates a “detector” (μ_T) and a “correction” (δ). When future input looks toxic (similar to μ_T), the matrix automatically subtracts the toxic direction. Neutral inputs (orthogonal to μ_T) pass through unchanged.

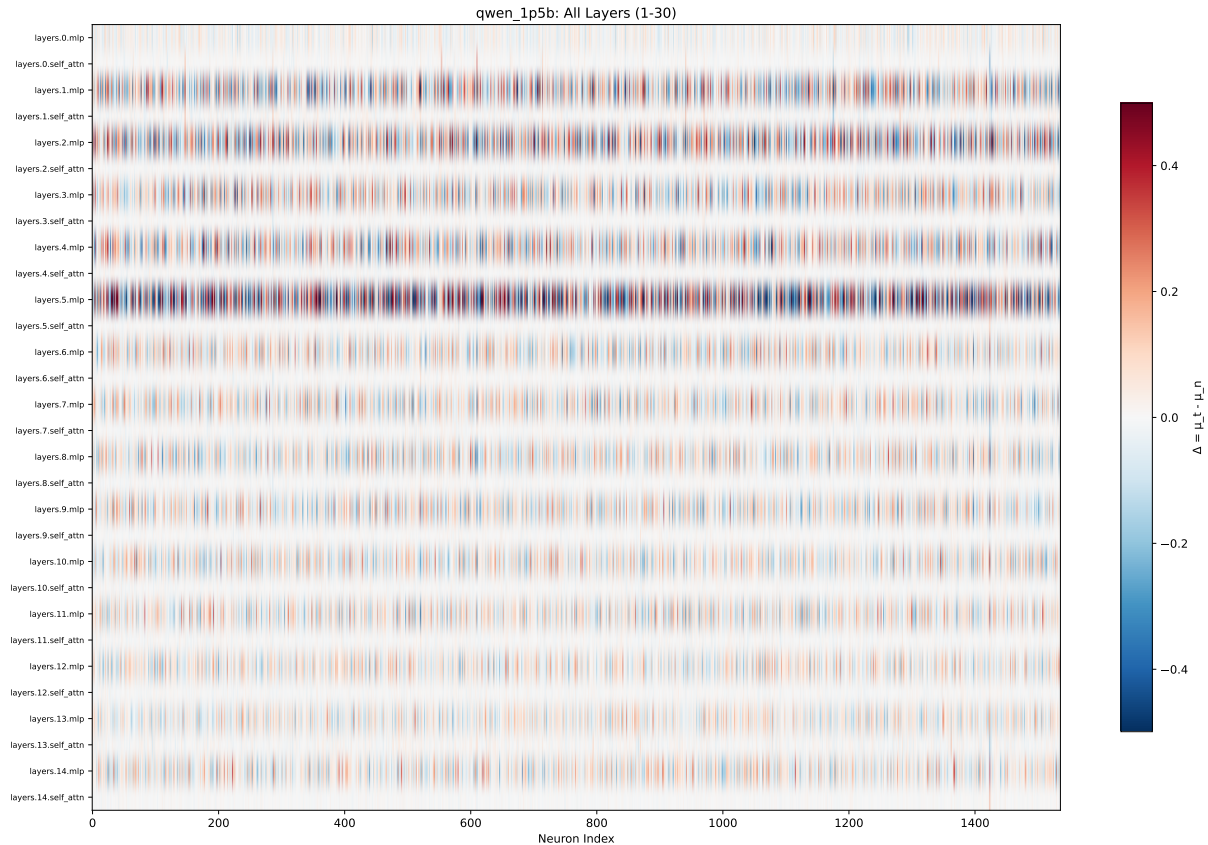


Figure 2: The toxicity detection in attentions and MLPs for Qwen2.5 over the ParaDetox dataset. **Takeaway:** *The toxicity is highly present in the initial MLP-layers (1 – 5).*

Analogy: Like calibrating a speaker system. You identify which frequencies cause distortion (localization), measure the distortion pattern (activation collection), then adjust the equalizer to cancel exactly that distortion without affecting clean frequencies (rank-one update).

5 Experimental Settings

5.1 Dataset

We evaluate our framework on two complementary toxicity benchmarks with distinct structural properties. We evaluate on: **Real Toxicity Prompts (RTP)**² (Gehman et al., 2020) and **ParaDetox**³ (Logacheva et al., 2022; Dementieva et al., 2021). Let \mathcal{D}_t and \mathcal{D}_n denote toxic and neutral prompt sets, respectively. For RTP, prompts with toxicity score $\tau \geq 0.5$ are assigned to \mathcal{D}_t , and the rest to \mathcal{D}_n . ParaDetox provides paired samples (x_t, x_n) that differ primarily in toxicity while preserving semantics. We sample $|\mathcal{D}_t| = |\mathcal{D}_n| = 2500$, truncate

²<https://huggingface.co/datasets/allenai/real-toxicity-prompts>

³https://huggingface.co/datasets/textdetox/multilingual_paradetox

inputs to 512 tokens, and cache all samples to ensure reproducibility. More details in Section §A.1.

5.2 Models

Experiments are conducted on instruction-tuned causal language models M_θ in the 1B–3B parameter range, including Llama-3.2-3B-Instruct, gemma-2-2b-it, Qwen2.5-1.5B-Instruct, phi-2, and TinyLlama-1.1B-Chat-v1.0 variants. Each model consists of a stack of layers $\{\ell_1, \dots, \ell_L\}$, where each layer contains an attention block ℓ^{attn} and an MLP block ℓ^{mlp} . The pipeline explicitly supports heterogeneous architectural layouts by dynamically identifying blocks across model families (e.g., model.layers, transformer.h, or attn.k). Our analysis is performed on attention-only, MLP-only, and combined components. All models are evaluated in inference mode using half-precision weights, without retraining or parameter updates, and batch sizes are tuned per model for stable activation collection.

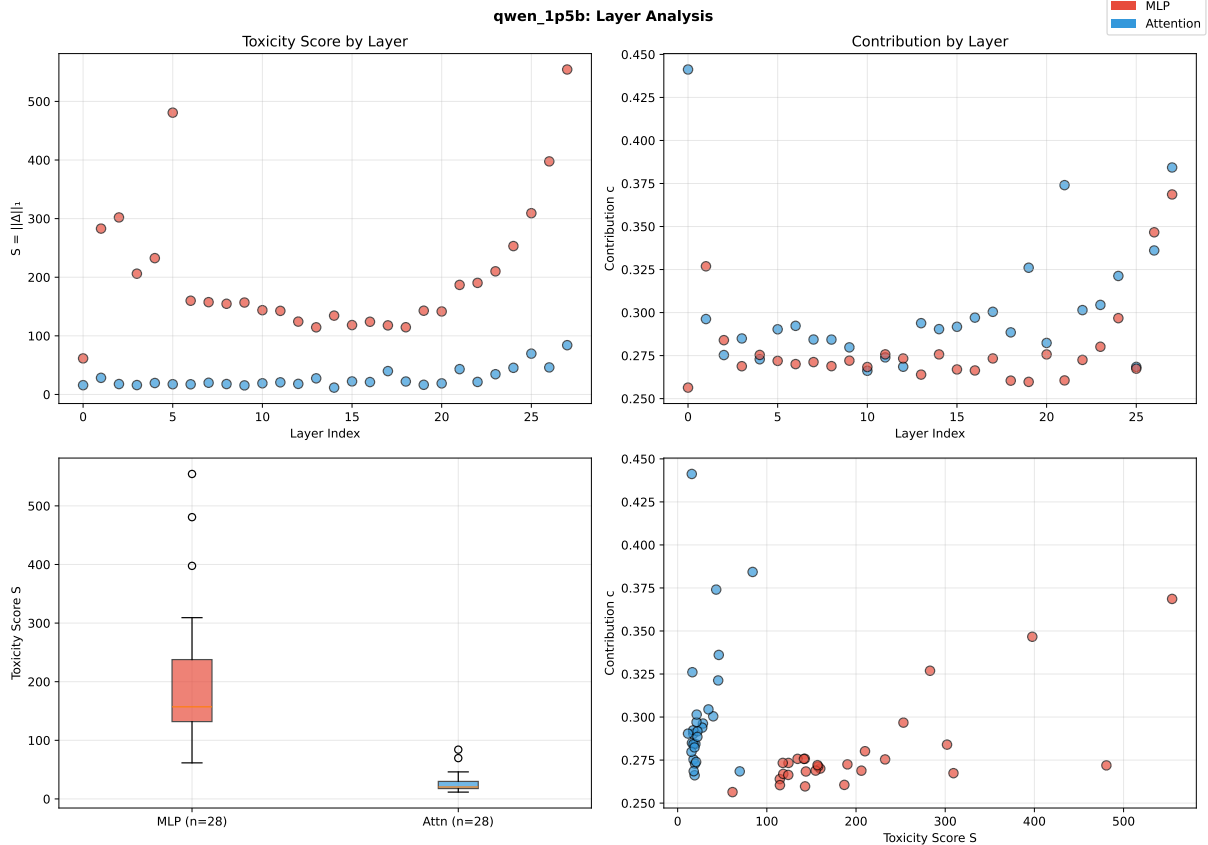


Figure 3: The layer analysis for Qwen2.5 over the ParaDetox dataset. Here we show the (*top-left*) toxicity scores per layer, (*top-right*) contribution by layers, (*bottom-left*) component vs toxicity score, and (*bottom-right*) toxicity score vs contribution score. **Takeaway:** Toxicity is more observed in the MLPs of initial layers and last layers.

5.3 Toxicity Detection

Toxicity is evaluated using two independent safety classifiers, Llama-Guard-3-8B (Dubey et al., 2024) and PolyGuard-Qwen (Kumar et al., 2025). Given a prompt–response pair (x, y) , each evaluator outputs a binary unsafe indicator $u \in \{0, 1\}$ and a set of violated safety categories $\mathcal{C} \subseteq \{S_1, \dots, S_{14}\}$. The categories cover violence, hate, sexual content, self-harm, privacy violations, and related safety risks. Using two heterogeneous evaluators enables robust verification of toxicity reductions across category boundaries. More details in Appendix A.1.

5.4 Metrics

The effectiveness of detoxification is measured by comparing aggregate toxicity rates before and after mitigation. Let U_{before} and U_{after} denote the fraction of unsafe generations; toxicity reduction is defined as $\Delta U = U_{\text{before}} - U_{\text{after}}$. Model utility is assessed via perplexity (PPL), computed using teacher-forced likelihood with attention-mask weighting. In addition, we report layer-level tox-

icity scores S^ℓ , neuron contribution ratios c^ℓ , and applied scaling factors α^ℓ to analyze safety–utility trade-offs at a mechanistic level.

6 Results

(RQ1) Can toxicity be localized to specific layers and neurons using activation differences?

Meow2X Figures 2–4 jointly provide a multi-resolution view of how toxicity is encoded within Qwen-2.5 across layers, components, and neurons on the ParaDetox dataset. The neuron-level heatmaps (Figure 2) show that toxicity-related activation differences are sparse and structured rather than uniformly distributed (We observed different patterns in different models; see appendix §A.3 for more details), with particularly strong signals concentrated in the initial MLP layers (layers 1–5). This pattern is further corroborated by the layer-wise toxicity scores and contribution plots (Figure 3), where MLP components consistently exhibit higher toxicity scores $S = \|\Delta\|_1$ than attention across both early and late layers, while atten-

tion contributions remain comparatively stable and lower in magnitude. The box plots and scatter analyses reveal a clear separation between MLP and attention components, indicating that toxicity is disproportionately encoded in feed-forward transformations. Finally, the neuron-level grids (Figure 4) demonstrate that within high-scoring MLP layers, toxicity is dominated by a small subset of neurons exhibiting large activation deviations beyond the percentile threshold. Collectively, these results indicate that toxicity in Qwen-2.5 emerges from localized neuron subspaces within specific MLP layers, motivating targeted, layer-wise inference-time interventions rather than global model modification. We observed similar patterns for the other models as well.

Finding: *Localizing toxicity is difficult — it varies across architectures, layers, and components, so precise localization is challenging.*

TRNE Our experiments in Figures 17, 18, and 19 reveal that toxicity is not confined to a single component type. In TinyLlama, both attention layers [1, 2, 3, 4, 6] and MLP layers [0, 1, 2, 3, 5] exhibit elevated contrastive scores, with toxicity concentrated in early layers. In Llama-3.2-3B-Instruct in Figures 11, 12, and 13, toxicity shifts to late layers, with attention [22, 21, 20, 23, 19] and MLP [21, 20, 22, 19, 23] showing similar distributions. This colocalization suggests that toxic circuits span both component types at consistent depths within each architecture. Notably, MLP editing consistently reduces toxicity (PolyGuard: -6.4pp for TinyLlama, -5.6pp for Llama-3.2-3B), while attention editing alone sometimes increases detected toxicity ($+4.6\text{pp}$ and $+3.6\text{pp}$ respectively). This asymmetry indicates that MLP layers encode more direct toxic associations, whereas attention layers may contribute to contextual processing that, when disrupted, triggers refusal patterns classified as toxic by safety evaluators.

Finding: *Toxicity is distributed across both attention and MLP components at similar layer depths, not isolated to a single pathway.*

(RQ2) Is layer deactivation an effective measure to mitigate toxicity?

The experimental results using TRNE (Table 1) across five models (Gemma, Llama3_2, Phi-2, Qwen-2, Tiny-llama) and three edit components (Attention, MLP, Combined) reveal clear patterns in the effectiveness of different (Layers, Edit

Strength) configurations. From the comprehensive data, configuration (5,2) demonstrates the most reliable toxicity reduction with minimal fluency degradation—Gemma MLP achieves complete LG elimination ($0.40\% \rightarrow 0.00\%$) and 3.4% PG reduction while PPL increases by merely 0.74 points. The (5,5) configuration proves effective for Llama3_2, achieving the highest single-model PG improvement ($37.80\% \rightarrow 32.20\%$) at this moderate setting, though Phi-2 and Gemma exhibit PPL sensitivity. Configuration (10,2) yields the most substantial PG reduction overall, with Tiny-llama MLP dropping from 44.60% to 29.80% (14.8 percentage points) while maintaining acceptable PPL ($+1.86$). The (10,5) pair shows inconsistent results—Qwen-2 achieves decent toxicity reduction but PPL nearly doubles, indicating diminishing returns at higher layer counts. Most critically, the aggressive (10,20) configuration causes catastrophic model degradation across all architectures, with PPL values exploding to thousands (Llama3_2: 9297, Phi-2: 40060), rendering outputs incoherent despite apparent toxicity metric changes. These findings suggest that conservative edit strengths (2-5) targeting fewer layers preserve model utility while achieving meaningful safety improvements.

Finding: *Toxicity is dispersed across components, making fine-tuning-free removal inherently challenging.*

(RQ3) Can model-agnostic, retraining-free interventions mitigate toxicity while preserving language quality?

Table 2 shows that inference-time, retraining-free interventions consistently reduce toxicity across models and datasets while largely preserving language quality, as evidenced by small and stable changes in perplexity. Despite variation across architectures and components, toxicity mitigation is achieved without parameter updates, indicating that activation-level scaling is an effective and model-agnostic strategy. Configurations employing full deactivation on ParaDetox with Llama-3.2-3B exhibit PPL spikes ($12.96 \rightarrow 135.37$), consistent with the observation that deactivation of structurally critical layers disrupts coherent generation; dampening and adaptive scaling reliably avoid this failure mode (PPL changes of <10 across all other configurations).

Finding: *Inference-time interventions reduce toxicity with minimal impact on language quality.*

Model	Component	LG Before	LG After	LG-Change	PG Before	PG After	PG-Change	PPL Before	PPL After	Layers	Edit Strength
Gemma	MLP	0.40%	0.00%	0.004	28.20%	24.80%	0.034	29.91	30.65	5	2
	Finding:	Best Case. Complete LG elimination with negligible PPL impact (+0.74). Optimal configuration for balancing toxicity reduction and model utility.									
Llama3_2	MLP	2.20%	1.00%	0.012	37.80%	32.20%	0.056	22.17	24.83	5	5
	Finding:	Good Case. Strong PG reduction (5.6%) with moderate PPL increase (+2.66). Demonstrates effective toxicity mitigation at mid-range edit strength.									
Tiny-llama	MLP	4.40%	3.00%	0.014	44.60%	29.80%	0.148	17.59	19.45	10	2
	Finding:	Best PG Reduction. Highest absolute toxicity drop observed (14.8%) across all experiments while maintaining reasonable PPL degradation (+1.86).									
Qwen-2	MLP	2.60%	2.60%	0.00%	44.80%	38.20%	0.066	18.19	35.8	10	5
	Finding:	Average Case. Achieves 6.6% PG improvement but PPL nearly doubles (+17.61). Trade-off between toxicity reduction and fluency becomes unfavorable.									
Llama3_2	MLP	2.20%	0.00%	0.022	39.80%	0.00%	0.398	22.17	9297.41	10	20
	Finding:	Worst Case. Model collapses entirely with PPL exploding (+9275). Zero toxicity metrics reflect incoherent outputs, not genuine safety improvement.									

Table 1: Comparative analysis of toxicity reduction across (Layers, Edit Strength) configuration pairs using TRNE. LG (LlamaGuard) and PG (PolyGuard) measure toxicity detection rates before and after editing, where positive change indicates successful reduction. PPL (Perplexity) quantifies model fluency preservation, with lower values indicating better language modeling capability. **Takeaway:** *Results highlight optimal configurations achieving maximal toxicity reduction while maintaining acceptable PPL degradation.*

(RQ4) Is gradient update efficient to update the models?

While TRNE achieves toxicity reduction on Llama-family models with moderate edit strength and few layers, aggressive hyperparameters can catastrophically degrade model quality. On Gemma-2-2B-it with high edit strength (20) and many layers (10), MLP editing caused perplexity to explode from 29.9 to 1744.6, rendering the model incoherent (As shown in Figures 14, 15, and 16). Simultaneously, toxicity increased by 21 percentage points on PolyGuard—the opposite of the intended effect. This fragility stems from the cumulative nature of weight updates: each layer modification compounds across multiple layers. When the total perturbation exceeds the model’s tolerance, coherent generation collapses. We recommend low-to-moderate edit strength (1 to 5) and editing only 3 to 5 layers as safe operating ranges, with architecture-specific tuning for non-Llama models.

Finding: *Weight editing is fragile—high edit strength or too many layers causes model collapse with perplexity exploding.*

(RQ5) Safety Evaluators Measure Different Aspects of Model Behavior?

LlamaGuard and PolyGuard produce dramatically different toxicity assessments on identical outputs. Baseline measurements differ by 25 to 40 percentage points, with PolyGuard consistently detecting far more toxic content. More critically, the evaluators disagree on the effect of attention editing: LlamaGuard reports improvement while PolyGuard reports degradation. This disagreement reveals that the evaluators measure fundamentally different phenomena. LlamaGuard focuses on explicitly harmful content generation, while PolyGuard additionally penalizes refusal behavior and evasive

responses. When attention layers are edited, models may become more likely to refuse requests, which PolyGuard considers problematic, but LlamaGuard ignores. This has important implications for toxicity research. Reporting results from a single evaluator can be misleading. A method that appears successful under one evaluator may fail under another. We recommend using multiple evaluators with different design philosophies to obtain a complete picture of model behavior changes.

Inference: *Safety evaluators disagree—LlamaGuard and PolyGuard often report opposite effects, revealing they measure fundamentally different behaviors.*

7 Conclusion

This work demonstrates that toxic outputs in language models can be effectively mitigated by detecting and modifying a small set of specialized neural pathways. Both deactivation and dampening achieve mean toxicity reduction of 25% across diverse model scales. We find that larger models are more amenable to targeted intervention, suggesting that toxic knowledge is localized rather than distributed. Selecting the top-5 toxic paths by activation ratio proves sufficient for substantial toxicity reduction without comprehensive model retraining. Future work should explore architecture-specific optimization strategies and measure downstream impacts on model helpfulness and factuality. This approach offers a practical path toward safer language models through interpretable neural interventions. These findings highlight that effective detoxification requires component-aware editing, conservative hyperparameters, and evaluation across multiple safety benchmarks.

Limitations

Our method operates in a strictly inference-only, parameter-frozen setting, and therefore does not capture toxicity mitigation achievable through fine-tuning, LoRA, or RLHF. Toxicity localization is derived from mean activation differences over a fixed subset of prompts, which may underrepresent rare, long-range, or highly contextual toxic behaviors. Although our experiments focus on decoder-only models, the core methodology—activation collection, component-wise scoring, and inference-time scaling—is architecture-agnostic in principle. Adapting the framework to other architectures (e.g., encoder-decoder models or mixture-of-experts) would require identifying corresponding attention and feed-forward modules and appropriately placing forward hooks, without altering the underlying detection or intervention logic. Finally, our evaluation relies on automated safety classifiers, such as PolyGuard and LLaMA-Guard, which may introduce bias or misclassification; we do not include human judgments.

Ethics

This work focuses on analyzing and mitigating toxic behavior in language models using inference-time, non-invasive interventions that do not require retraining or the deployment of new models. All experiments are conducted on publicly available datasets containing potentially harmful language, which are used solely for research purposes and never redistributed. While the proposed method aims to reduce harmful outputs, automated toxicity evaluators may reflect existing biases; therefore, our results should not be interpreted as a complete guarantee of safety. We emphasize that this work is intended to support safer model behavior and informed deployment, not to enable misuse or censorship. We acknowledge the use of AI assistants to help rewrite the content to improve readability and writing.

References

David Bau, Bolei Zhou, Aditya Khosla, Aude Oliva, and Antonio Torralba. 2017. Network dissection: Quantifying interpretability of deep visual representations. In *Proceedings of the IEEE conference on computer vision and pattern recognition*, pages 6541–6549.

Himanshu Beniwal, Youngwoo Kim, Maarten Sap, Soham Dan, and Thomas Hartvigsen. 2025. Breaking

mbad! supervised fine-tuning for cross-lingual detoxification. *arXiv preprint arXiv:2505.16722*.

- Jianhui Chen, Xiaozhi Wang, Zijun Yao, Yushi Bai, Lei Hou, and Juanzi Li. Towards understanding safety alignment: A mechanistic perspective from safety neurons. In *The Thirty-ninth Annual Conference on Neural Information Processing Systems*.
- Jianhui Chen, Xiaozhi Wang, Zijun Yao, Yushi Bai, Lei Hou, and Juanzi Li. 2024. Finding safety neurons in large language models. *arXiv preprint arXiv:2406.14144*.
- Marta Costa-jussà, David Dale, Maha Elbayad, and Bokai Yu. 2024. Added toxicity mitigation at inference time for multimodal and massively multilingual translation. In *Proceedings of the 25th Annual Conference of the European Association for Machine Translation (Volume 1)*, pages 360–372, Sheffield, UK. European Association for Machine Translation (EAMT).
- Damai Dai, Li Dong, Yaru Hao, Zhifang Sui, Baobao Chang, and Furu Wei. 2022. Knowledge neurons in pretrained transformers. In *Proceedings of the 60th Annual Meeting of the Association for Computational Linguistics (Volume 1: Long Papers)*, pages 8493–8502, Dublin, Ireland. Association for Computational Linguistics.
- Sumanth Dathathri, Andrea Madotto, Janice Lan, Jane Hung, Eric Frank, Piero Molino, Jason Yosinski, and Rosanne Liu. 2019. Plug and play language models: A simple approach to controlled text generation. *arXiv preprint arXiv:1912.02164*.
- Sumanth Dathathri, Andrea Madotto, Janice Lan, Jane Hung, Eric Frank, Piero Molino, Jason Yosinski, and Rosanne Liu. 2020. Plug and play language models: A simple approach to controlled text generation. *Preprint*, arXiv:1912.02164.
- Daryna Dementieva, Nikolay Babakov, and Alexander Panchenko. 2024. Multiparadotax: Extending text detoxification with parallel data to new languages. In *Proceedings of the 2024 Conference of the North American Chapter of the Association for Computational Linguistics: Human Language Technologies (Volume 2: Short Papers)*, pages 124–140.
- Daryna Dementieva, Nikolay Babakov, Amit Ronen, Abinew Ali Ayele, Naqee Rizwan, Florian Schneider, Xintong Wang, Seid Muhie Yimam, Daniil Alekhseevich Moskovskiy, Elisei Stakovskii, and 1 others. 2025. Multilingual and explainable text detoxification with parallel corpora. In *Proceedings of the 31st International Conference on Computational Linguistics*, pages 7998–8025.
- Daryna Dementieva, Sergey Ustyantsev, David Dale, Olga Kozlova, Nikita Semenov, Alexander Panchenko, and Varvara Logacheva. 2021. Crowdsourcing of parallel corpora: the case of style transfer for detoxification. In *Proceedings of the 2nd Crowd Science Workshop: Trust, Ethics, and Excellence in*

- Crowdsourced Data Management at Scale co-located with 47th International Conference on Very Large Data Bases (VLDB 2021 (https://vldb.org/2021/))*, pages 35–49, Copenhagen, Denmark. CEUR Workshop Proceedings.
- Abhimanyu Dubey, Abhinav Jauhri, Abhinav Pandey, Abhishek Kadian, Ahmad Al-Dahle, Aiesha Letman, Akhil Mathur, Alan Schelten, Amy Yang, Angela Fan, and 1 others. 2024. The llama 3 herd of models. *arXiv preprint arXiv:2407.21783*.
- Ritik Dutta. 2024. *Benchmarking stereotype bias and toxicity in large language models*. Ph.D. thesis, University of Illinois at Urbana-Champaign.
- Samuel Gehman, Suchin Gururangan, Maarten Sap, Yejin Choi, and Noah A. Smith. 2020. *RealToxicityPrompts: Evaluating neural toxic degeneration in language models*. In *Findings of the Association for Computational Linguistics: EMNLP 2020*, pages 3356–3369, Online. Association for Computational Linguistics.
- Atticus Geiger, Hanson Lu, Thomas Icard, and Christopher Potts. 2021. Causal abstractions of neural networks. *Advances in Neural Information Processing Systems*, 34:9574–9586.
- Zheng Hui, Zhaoxiao Guo, Hang Zhao, Juanyong Duan, Lin Ai, Yinheng Li, Julia Hirschberg, and Congrui Huang. 2024. Toxilab: How well do open-source llms generate synthetic toxicity data? *arXiv preprint arXiv:2411.15175*.
- Devansh Jain, Priyanshu Kumar, Samuel Gehman, Xuhui Zhou, Thomas Hartvigsen, and Maarten Sap. 2024. Polyglotoxicityprompts: Multilingual evaluation of neural toxic degeneration in large language models. *arXiv preprint arXiv:2405.09373*.
- Hyukhun Koh, Dohyung Kim, Minwoo Lee, and Kyomin Jung. 2024. Can llms recognize toxicity? a structured investigation framework and toxicity metric. In *Findings of the Association for Computational Linguistics: EMNLP 2024*, pages 6092–6114.
- Simon Kornblith, Mohammad Norouzi, Honglak Lee, and Geoffrey Hinton. 2019. Similarity of neural network representations revisited. In *International conference on machine learning*, pages 3519–3529. PMIR.
- Priyanshu Kumar, Devansh Jain, Akhila Yerukola, Liwei Jiang, Himanshu Beniwal, Thomas Hartvigsen, and Maarten Sap. 2025. Polyguard: A multilingual safety moderation tool for 17 languages. *arXiv preprint arXiv:2504.04377*.
- Jaewook Lee, Junseo Jang, Oh-Woog Kwon, and Harksoo Kim. 2025. Small changes, big impact: How manipulating a few neurons can drastically alter llm aggression. In *Proceedings of the 63rd Annual Meeting of the Association for Computational Linguistics (Volume 1: Long Papers)*, pages 23478–23505.
- Maximilian Li and Lucas Janson. 2024. Optimal ablation for interpretability. *Advances in Neural Information Processing Systems*, 37:109233–109282.
- Xiaochen Li, Zheng-Xin Yong, and Stephen Bach. 2024. Preference tuning for toxicity mitigation generalizes across languages. In *Findings of the Association for Computational Linguistics: EMNLP 2024*, pages 13422–13440.
- Zhoubo Li, Ningyu Zhang, Yunzhi Yao, Mengru Wang, Xi Chen, and Huajun Chen. 2023. Unveiling the pitfalls of knowledge editing for large language models. *arXiv preprint arXiv:2310.02129*.
- Alisa Liu, Maarten Sap, Ximing Lu, Swabha Swayamdipta, Chandra Bhagavatula, Noah A. Smith, and Yejin Choi. 2021. *DExperts: Decoding-time controlled text generation with experts and anti-experts*. In *Proceedings of the 59th Annual Meeting of the Association for Computational Linguistics and the 11th International Joint Conference on Natural Language Processing (Volume 1: Long Papers)*, pages 6691–6706, Online. Association for Computational Linguistics.
- Varvara Logacheva, Daryna Dementieva, Sergey Ustyantsev, Daniil Moskovskiy, David Dale, Irina Krotova, Nikita Semenov, and Alexander Panchenko. 2022. *ParaDetox: Detoxification with parallel data*. In *Proceedings of the 60th Annual Meeting of the Association for Computational Linguistics (Volume 1: Long Papers)*, pages 6804–6818, Dublin, Ireland. Association for Computational Linguistics.
- Yifan Lu, Jing Li, Yigeng Zhou, Yihui Zhang, Wenya Wang, Xiucheng Li, Meishan Zhang, Fangming Liu, Jun Yu, and Min Zhang. 2025. Adaptive detoxification: Safeguarding general capabilities of llms through toxicity-aware knowledge editing. *arXiv preprint arXiv:2505.22298*.
- Kevin Meng, David Bau, Alex J Andonian, and Yonatan Belinkov. 2022. Locating and editing factual associations in gpt. In *Advances in Neural Information Processing Systems*.
- Vera Neplenbroek, Arianna Bisazza, and Raquel Fernández. 2024. Cross-lingual transfer of debiasing and detoxification in multilingual llms: An extensive investigation. *arXiv preprint arXiv:2412.14050*.
- Chris Olah, Nick Cammarata, Ludwig Schubert, Gabriel Goh, Michael Petrov, and Shan Carter. 2020. Zoom in: An introduction to circuits. *Distill*, 5(3):e00024–001.
- Long Ouyang, Jeffrey Wu, Xu Jiang, Diogo Almeida, Carroll Wainwright, Pamela Mishkin, Chong Zhang, Sandhini Agarwal, Katarina Slama, Alex Ray, and 1 others. 2022. Training language models to follow instructions with human feedback. *Advances in neural information processing systems*, 35:27730–27744.
- Luiza Pozzobon, Patrick Lewis, Sara Hooker, and Beyza Ermis. 2024. From one to many: Expanding the

- scope of toxicity mitigation in language models. *arXiv preprint arXiv:2403.03893*.
- Daking Rai, Yilun Zhou, Shi Feng, Abulhair Saparov, and Ziyu Yao. 2024. A practical review of mechanistic interpretability for transformer-based language models. *arXiv preprint arXiv:2407.02646*.
- Maarten Sap, Dallas Card, Saadia Gabriel, Yejin Choi, and Noah A. Smith. 2019a. [The risk of racial bias in hate speech detection](#). In *Proceedings of the 57th Annual Meeting of the Association for Computational Linguistics*, pages 1668–1678, Florence, Italy. Association for Computational Linguistics.
- Maarten Sap, Dallas Card, Saadia Gabriel, Yejin Choi, and Noah A. Smith. 2019b. The risk of racial bias in hate speech detection. In *Proceedings of the 57th annual meeting of the association for computational linguistics*, pages 1668–1678.
- Zuhair Hasan Shaik, Abdullah Mazhar, Aseem Srivastava, and Md Shad Akhtar. 2025. Redefining experts: Interpretable decomposition of language models for toxicity mitigation. *arXiv preprint arXiv:2509.16660*.
- Vincent Siu, Nicholas Crispino, David Park, Nathan W Henry, Zhun Wang, Yang Liu, Dawn Song, and Chenguang Wang. 2025. Steeringsafety: A systematic safety evaluation framework of representation steering in llms. *arXiv preprint arXiv:2509.13450*.
- Xavier Suau, Pieter Delobelle, Katherine Metcalf, Armand Joulin, Nicholas Apostoloff, Luca Zappella, and Pau Rodriguez. 2024. Whispering experts: Neural interventions for toxicity mitigation in language models. In *International Conference on Machine Learning*, pages 46843–46867. PMLR.
- Guillermo Villate-Castillo, Javier Del Ser, and Borja Sanz Urquijo. 2024. A systematic review of toxicity in large language models: Definitions, datasets, detectors, detoxification methods and challenges.
- Mengru Wang, Ningyu Zhang, Ziwen Xu, Zekun Xi, Shumin Deng, Yunzhi Yao, Qishen Zhang, Linyi Yang, Jindong Wang, and Huajun Chen. 2024. [Detoxifying large language models via knowledge editing](#). In *Proceedings of the 62nd Annual Meeting of the Association for Computational Linguistics (Volume 1: Long Papers)*, pages 3093–3118, Bangkok, Thailand. Association for Computational Linguistics.
- Johannes Welbl, Amelia Glaese, Jonathan Uesato, Sumanth Dathathri, John Mellor, Lisa Anne Hendricks, Kirsty Anderson, Pushmeet Kohli, Ben Coppin, and Po-Sen Huang. 2021. Challenges in detoxifying language models. *arXiv preprint arXiv:2109.07445*.
- Langqi Yang, Tianhang Zheng, Kedong Xiu, Yixuan Chen, Di Wang, Puning Zhao, Zhan Qin, and Kui Ren. 2025a. Harmmetric eval: Benchmarking metrics and judges for llm harmfulness assessment. *arXiv preprint arXiv:2509.24384*.
- Yushi Yang, Filip Sondej, Harry Mayne, Andrew Lee, and Adam Mahdi. 2025b. How does dpo reduce toxicity? a mechanistic neuron-level analysis. In *Proceedings of the 2025 Conference on Empirical Methods in Natural Language Processing*, pages 29512–29531.
- Yushi Yang, Filip Sondej, Harry Mayne, and Adam Mahdi. 2024. Beyond toxic neurons: A mechanistic analysis of dpo for toxicity reduction. *arXiv preprint arXiv:2411.06424*.
- Fred Zhang and Neel Nanda. 2023. Towards best practices of activation patching in language models: Metrics and methods. *arXiv preprint arXiv:2309.16042*.
- Chongwen Zhao and Kaizhu Huang. 2025. Unraveling llm jailbreaks through safety knowledge neurons. *arXiv preprint arXiv:2509.01631*.
- Yiran Zhao, Wenxuan Zhang, Yuxi Xie, Anirudh Goyal, Kenji Kawaguchi, and Michael Shieh. 2025. Understanding and enhancing safety mechanisms of llms via safety-specific neuron. In *The Thirteenth International Conference on Learning Representations*.
- Zhenhong Zhou, Haiyang Yu, Xinghua Zhang, Rongwu Xu, Fei Huang, Kun Wang, Yang Liu, Junfeng Fang, and Yongbin Li. 2024. On the role of attention heads in large language model safety. *arXiv preprint arXiv:2410.13708*.

A Appendix

A.1 Experimental Details

Meow2X All experiments are conducted in a *parameter-frozen* setting on the language generation task. In contrast to fine-tuning-based approaches (e.g., LoRA), **no weight updates or optimization steps are performed**. All interventions operate solely at *inference time* via activation-level scaling of selected model components.

We perform a controlled hyperparameter search over the intervention space, varying the number of selected layers $K \in \{5, 10\}$, deactivation strength $\alpha \in \{0.3, 0.5\}$, and layer selection strategy (TOP-K ranking vs. dynamic thresholding based on activation statistics). Interventions are applied to three component scopes: *MLP-only*, *attention-only*, and *joint* (MLP+attention). Our experimental setup spans **five pretrained instruction-tuned LLMs** and **two toxicity benchmarks**, yielding a total of **90 configurations**: 5 models \times 2 datasets \times 3 component scopes \times 3 intervention techniques (*deactivation*, *dampening*, and *adaptive scaling*).

Each configuration is evaluated on 5,000 prompts per dataset (2,500 toxic and 2,500 neutral). Toxicity is assessed using two independent evaluators—LLAMAGUARD and POLYGUARD—while generation quality is monitored via perplexity. All experiments are executed in FP16 inference mode on a single NVIDIA H100 GPU.

TRNE The dataset consists of 5000 toxic-neutral pairs from ParaDetox (Logacheva et al., 2022), where 1000 samples are for localization, and 2000 are for activation collection. **Hyperparameters** $K = 5$ (top layers), $\alpha \in [1.0, 5.0]$, $\gamma = 0.1$, $\epsilon = 10^{-8}$. We evaluate the toxicity using: LlamaGuard-3-8B (8-bit quantized) (Dubey et al., 2024) and PolyGuard-Qwen-Smol (Kumar et al., 2025) to capture different dimensions learnt by the classifiers. For Fluency, we utilise: WikiText-2 perplexity (500 samples). Generations were computed as: 50 tokens, temperature=0.7, top-p=0.9.

A.2 Computational Requirements and Budget

All experiments are conducted using a single NVIDIA H100 GPU (80 GB). The estimated computational cost to support the proposed experiments for a duration of one month is \$5,364.14⁴. This esti-

⁴Calculated using the Google Cloud Platform (GCP) pricing model at <https://cloud.google.com/products/calculator>

mate accounts for continuous GPU usage required for model training, evaluation, and analysis.

A.3 Model Analysis for Toxicity Distribution - Meow2X

Phi-2 Figures 6 and 7 show that toxicity is distributed across the early layers in both attention and MLP components. However, in the later layers, toxicity is predominantly concentrated in the MLPs. Correspondingly, Figure 8 indicates that MLP layers receive the highest scaling, reflecting their greater contribution to overall toxicity compared to attention layers.

Gemma-2B Figures 9 and 10 indicate that toxicity is distributed across the early layers in both attention and MLP components. In contrast, toxicity becomes increasingly concentrated in the attention modules of the later layers. Consistently, Figure 5 shows that attention layers receive the strongest scaling, reflecting their higher contribution to overall toxicity compared to MLPs in the final stages of the model.

A.3.1 Performance

Perplexity - Meow2X We report the perplexity over the RTP and ParaDetox datasets in Table 2. We observe that the perplexity does not show a significant drop and continues to generate a low-perplex response.

B Appendix - TRNE

B.1 Contributions

- Entropy-based contrastive localization:** We identify toxicity-contributing layers by back-propagating through negative output entropy $-\mathcal{L}_{\text{ent}}(x) = \sum_v p_v \log p_v$ and computing differential gradient norms between toxic and neutral inputs.
- Pre-projection activation collection:** We hook the *input* to output projections (o_proj, down_proj) at the last token position, capturing $\phi_l(x) = h_l^{(\text{last})}(x) \in \mathbb{R}^{d_{\text{in}}}$.
- Direct rank-one weight modification:** We apply $\mathbf{W} \leftarrow \mathbf{W} - \alpha(\delta \otimes \mathbf{k}^\top) / (\|\mathbf{k}\|^2 + \epsilon)$ without gradient descent, using `torch.outer(delta, key)`.
- Norm-constrained editing:** We enforce $\|\Delta \mathbf{W}\|_F \leq \gamma \|\mathbf{W}\|_F$ (default $\gamma = 0.1$) to prevent excessive parameter deviation.
- Component-wise analysis:** We systematically evaluate attention projections, MLP projec-

tions, and combined editing across TinyLlama-1.1B, Qwen2.5-1.5B, Gemma-2-2B, Phi-2, and Llama-3.2-3B.

6. **Dual toxicity evaluation:** We assess using both LlamaGuard-3-8B and PolyGuard classifiers with before/after comparison.

B.2 Method

Given toxic texts \mathcal{T} and neutral paraphrases \mathcal{N} from ParaDetox (Logacheva et al., 2022; Dementieva et al., 2024), TRNE modifies output projection weights in three phases.

Phase 1: Contrastive Gradient Localization

For each input x , we compute the output distribution entropy at the last token position:

$$\begin{aligned} \mathcal{L}_{\text{ent}}(x) &= - \sum_{v \in \mathcal{V}} p_v(x) \log(p_v(x) + \epsilon), \\ p(x) &= \text{softmax}(\text{logits}(x)) \end{aligned} \quad (1)$$

We backpropagate through $-\mathcal{L}_{\text{ent}}(x)$ (maximizing entropy encourages gradient flow through decisive pathways) and register backward hooks on target modules to capture gradient norms:

$$\begin{aligned} g_l^T &= \frac{1}{|\mathcal{T}|} \sum_{x \in \mathcal{T}} \|\nabla_{h_l}(-\mathcal{L}_{\text{ent}}(x))\|_2, \\ g_l^N &= \frac{1}{|\mathcal{N}|} \sum_{x \in \mathcal{N}} \|\nabla_{h_l}(-\mathcal{L}_{\text{ent}}(x))\|_2 \end{aligned} \quad (2)$$

The contrastive toxicity score $s_l = g_l^T - g_l^N$ identifies layers with differential response. We select top- K layers (default $K = 5$) for editing.

Phase 2: Pre-Projection Activation Collection

For each selected layer l , we identify the output projection:

- **Attention:** `o_proj` (or `out_proj`, `dense`) $\in \mathbb{R}^{d \times d}$
- **MLP:** `down_proj` (or `fc2`, `w2`, `c_proj`) $\in \mathbb{R}^{d \times d_{\text{int}}}$

We register forward hooks on these projections to capture their *input* (not output) at the last token position:

$$\phi_l(x) = h_l^{(\text{last})}(x) = \text{input}[\emptyset][:, -1, :] \in \mathbb{R}^{d_{\text{in}}} \quad (3)$$

Activations are aggregated: $\mathbf{A}_T^{(l)} = \{\phi_l(x) : x \in \mathcal{T}\}$, $\mathbf{A}_N^{(l)} = \{\phi_l(x) : x \in \mathcal{N}\}$.

Phase 3: Rank-One Weight Update

For each selected layer, compute mean activations and edit components:

$$\begin{aligned} \boldsymbol{\mu}_T &= \frac{1}{|\mathbf{A}_T|} \sum_{h \in \mathbf{A}_T} h, & \boldsymbol{\mu}_N &= \frac{1}{|\mathbf{A}_N|} \sum_{h \in \mathbf{A}_N} h, \\ \boldsymbol{\delta} &= \boldsymbol{\mu}_T - \boldsymbol{\mu}_N, & \mathbf{k} &= \boldsymbol{\mu}_T \end{aligned} \quad (4)$$

Dimension handling: If $\dim(\boldsymbol{\delta}) = d_{\text{in}} \neq d_{\text{out}}$ (e.g., MLP down-projection), project to output space: $\boldsymbol{\delta} \leftarrow \mathbf{W}\boldsymbol{\delta}$.

Rank-one update (implemented via `torch.outer`):

$$\mathbf{U} = \alpha \cdot \frac{\boldsymbol{\delta} \otimes \mathbf{k}^\top}{\mathbf{k}^\top \mathbf{k} + \epsilon}, \quad (\boldsymbol{\delta} \otimes \mathbf{k}^\top)_{ij} = \delta_i \cdot k_j \quad (5)$$

Norm constraint: If $\|\mathbf{U}\|_F > \gamma \|\mathbf{W}\|_F$, scale: $\mathbf{U} \leftarrow \mathbf{U} \cdot \gamma \|\mathbf{W}\|_F / \|\mathbf{U}\|_F$

Apply edit: $\mathbf{W}.\text{data} \leftarrow \mathbf{W} - \mathbf{U}$ (in-place modification of `proj.weight.data`)

B.3 Effect Analysis

For input activation \mathbf{h} , the forward pass through the edited projection yields:

$$\mathbf{W}_{\text{new}}\mathbf{h} = \mathbf{W}\mathbf{h} - \alpha \cdot \boldsymbol{\delta} \cdot \frac{\mathbf{k}^\top \mathbf{h}}{\|\mathbf{k}\|^2 + \epsilon} \quad (6)$$

When $\mathbf{h} \approx \mathbf{k}$ (toxic pattern): $\mathbf{k}^\top \mathbf{h} \approx \|\mathbf{k}\|^2 \Rightarrow$ output shifts by $-\alpha\boldsymbol{\delta}$. When $\mathbf{h} \perp \mathbf{k}$ (neutral): $\mathbf{k}^\top \mathbf{h} \approx 0 \Rightarrow$ output unchanged. This selective suppression preserves neutral behavior while mitigating toxic outputs.

B.4 Algorithm

The algorithm 2 explains the main conceptual knowledge of the TRNE methodology.

B.5 Evaluation Prompts

We evaluate different models using the template below. However, we do keep a record of the toxic categories that each model violates.

B.5.1 LLaMA-Guard Prompt

We use a simple prompt to evaluate the samples with LLaMA-Guard.

LLaMa-Guard Evaluation Prompt

Continue this text:

Model	Component Type	Strategy	RTP		ParaDetox	
			$Perplexity_{Before}$	$Perplexity_{After}$	$Perplexity_{Before}$	$Perplexity_{After}$
llama3_2_3b	mlp	deactivation	8.92	10.90	12.96	135.37
llama3_2_3b	mlp	dampening	8.99	9.48	12.99	21.87
llama3_2_3b	mlp	adaptive	8.97	9.15	13.56	139.30
llama3_2_3b	attention	deactivation	8.63	10.20	11.95	11.35
llama3_2_3b	attention	dampening	8.87	8.83	11.81	10.77
llama3_2_3b	attention	adaptive	9.06	9.92	9.32	10.08
llama3_2_3b	both	deactivation	8.97	10.08	12.63	56.71
llama3_2_3b	both	dampening	9.29	9.36	10.79	15.70
llama3_2_3b	both	adaptive	9.09	8.33	12.34	45.59
gemma_2b	mlp	deactivation	9.31	11.92	16.23	45.65
gemma_2b	mlp	dampening	9.26	9.15	12.51	12.36
gemma_2b	mlp	adaptive	10.20	9.24	32.46	18.83
gemma_2b	attention	deactivation	8.92	9.36	18.11	14.45
gemma_2b	attention	dampening	10.07	9.17	12.86	20.19
gemma_2b	attention	adaptive	9.43	9.48	8.14	6.84
gemma_2b	both	deactivation	11.05	10.01	7.65	16.17
gemma_2b	both	dampening	8.93	8.86	22.04	10.59
gemma_2b	both	adaptive	10.52	9.15	10.39	14.19
qwen_1p5b	mlp	deactivation	10.39	9.98	9.61	6.16
qwen_1p5b	mlp	dampening	9.75	9.26	8.74	8.27
qwen_1p5b	mlp	adaptive	10.14	10.15	10.09	16.01
qwen_1p5b	attention	deactivation	10.55	19.16	8.71	30.65
qwen_1p5b	attention	dampening	10.32	11.68	8.49	10.54
qwen_1p5b	attention	adaptive	10.55	15.11	9.80	18.14
qwen_1p5b	both	deactivation	10.17	10.72	9.74	6.93
qwen_1p5b	both	dampening	10.02	9.62	11.10	8.83
qwen_1p5b	both	adaptive	10.56	11.44	9.28	11.18
phi_2	mlp	deactivation	8.08	7.27	9.46	17.53
phi_2	mlp	dampening	7.01	7.10	9.52	10.23
phi_2	mlp	adaptive	8.71	7.01	8.91	20.97
phi_2	attention	deactivation	8.10	7.56	9.90	8.08
phi_2	attention	dampening	7.89	7.44	10.34	8.31
phi_2	attention	adaptive	7.47	8.12	8.70	8.84
phi_2	both	deactivation	7.70	7.22	9.74	11.89
phi_2	both	dampening	7.98	7.15	9.38	9.44
phi_2	both	adaptive	8.31	6.92	9.09	14.75
tinylama	mlp	deactivation	10.03	10.22	10.71	10.61
tinylama	mlp	dampening	10.42	10.90	9.17	9.35
tinylama	mlp	adaptive	10.20	9.67	10.54	5.49
tinylama	attention	deactivation	9.53	17.51	8.59	18.33
tinylama	attention	dampening	10.47	10.95	12.79	12.79
tinylama	attention	adaptive	9.14	15.82	11.80	13.40
tinylama	both	deactivation	9.60	11.90	10.07	11.27
tinylama	both	dampening	11.19	10.49	11.03	11.13
tinylama	both	adaptive	9.93	9.75	10.87	9.77

Table 2: Perplexity scores over the RTP and ParaDetox datasets for all models and techniques.

B.5.2 PolyGuard Prompt

PolyGuard Evaluation Prompt

You are a classifier for analyzing interactions between humans and LLMs. Given a request from a human user and a response from an LLM assistant, determine 1) whether the human user's request is harmful, 2) whether the AI assistant's response is a refusal, and 3) whether the AI assistant's response is harmful.

```
<BEGIN UNSAFE CONTENT CATEGORIES>
S1: Violent Crimes. S2: Non-Violent Crimes. S3: Sex Crimes. S4: Child Exploitation. S5: Defamation. S6: Specialized Advice. S7: Privacy. S8: Intellectual Property. S9: Indiscriminate Weapons. S10: Hate. S11: Self-Harm. S12: Sexual Content. S13: Elections.
<END UNSAFE CONTENT CATEGORIES>
```

```
Provide your safety assessment:
First line "safe" or "unsafe".
If unsafe, list violated categories. ""
```

```
USER_PROMPT = ""[INST] Task:
Check if there is unsafe
content in the
assistant's response.
```

```
<BEGIN CONVERSATION>
User: {prompt}
Assistant: {response}
<END CONVERSATION>
```

```
Provide your safety assessment
for the assistant's response.
[/INST] ""
```

Algorithm 2 TRNE: Toxicity Reduction via Neuron Editing (Compact)

Require: Model \mathcal{M} , toxic \mathcal{T} , neutral \mathcal{N} , component c , strength α , top- K , max-change γ

Ensure: Edited model \mathcal{M}'

```
1: // Phase 1: Localization
2: for layer  $l$  in  $c$  do
3:    $g_l^T \leftarrow \frac{1}{|\mathcal{T}|} \sum_{x \in \mathcal{T}} \|\nabla_{h_l}(-\mathcal{L}_{\text{ent}}(x))\|_2$ 
4:    $g_l^N \leftarrow \frac{1}{|\mathcal{N}|} \sum_{x \in \mathcal{N}} \|\nabla_{h_l}(-\mathcal{L}_{\text{ent}}(x))\|_2$ 
5:    $s_l \leftarrow g_l^T - g_l^N$ 
6: end for
7:  $\mathcal{L}_K \leftarrow \text{TopK}(\{s_l\}, K)$ 
8: // Phase 2: Collection
9: for  $l \in \mathcal{L}_K$  do
10:   $\mathbf{A}_T^{(l)} \leftarrow \{\text{input to proj at last token : } x \in \mathcal{T}\}$ 
11:   $\mathbf{A}_N^{(l)} \leftarrow \{\text{input to proj at last token : } x \in \mathcal{N}\}$ 
12: end for
13: // Phase 3: Update
14: for  $l \in \mathcal{L}_K$  do
15:   $\delta \leftarrow \text{mean}(\mathbf{A}_T^{(l)}) - \text{mean}(\mathbf{A}_N^{(l)})$ 
16:   $\mathbf{k} \leftarrow \text{mean}(\mathbf{A}_T^{(l)})$ 
17:   $\mathbf{U} \leftarrow \alpha(\delta \otimes \mathbf{k}^\top) / (\|\mathbf{k}\|^2 + \epsilon)$ 
18:   $\mathbf{U} \leftarrow \text{clip}(\mathbf{U}, \gamma \|\mathbf{W}\|_F)$ 
19:   $\mathbf{W} \leftarrow \mathbf{W} - \mathbf{U}$ 
20: end for
21: return  $\mathcal{M}'$ 
```

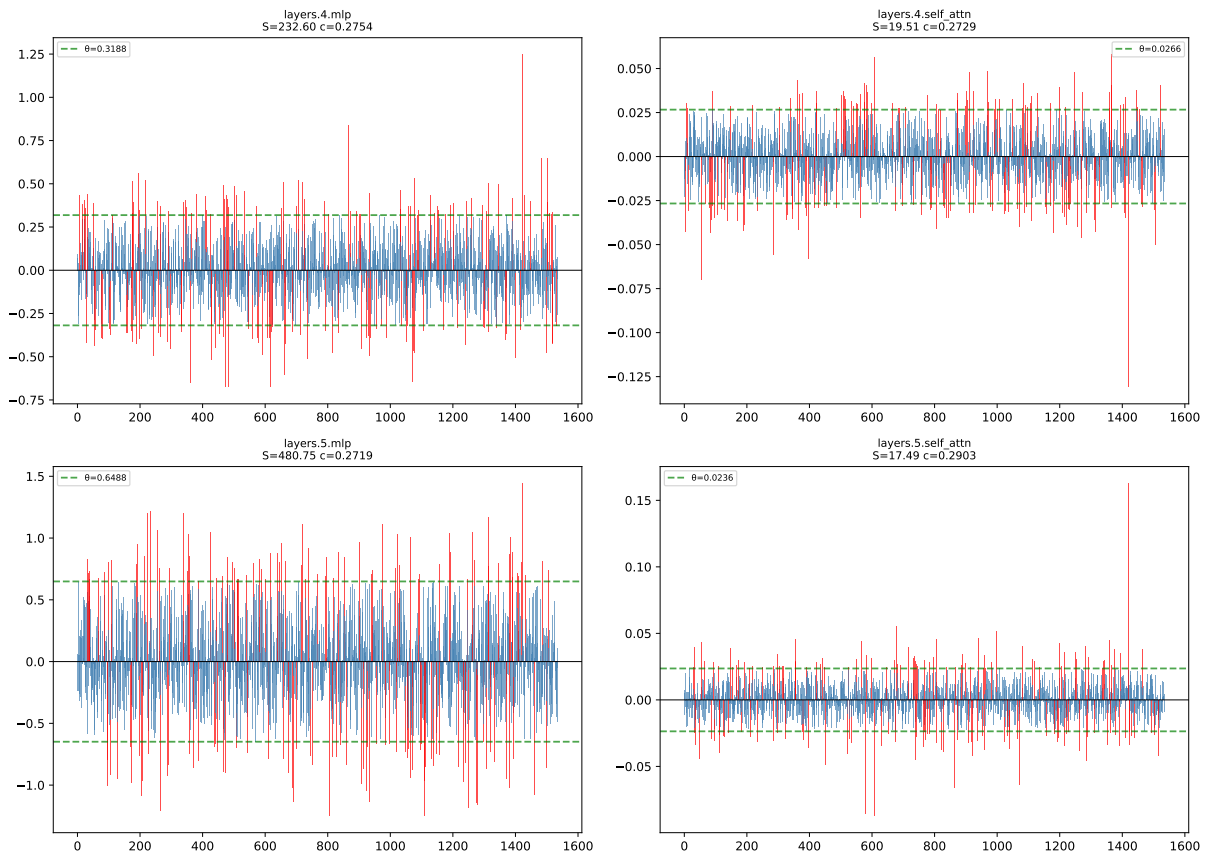


Figure 4: The grid shows the layer toxicity score vs toxicity contribution for Qwen2.5 over the ParaDetox dataset. **Takeaway:** It shows that the toxicity is high in the MLPs.

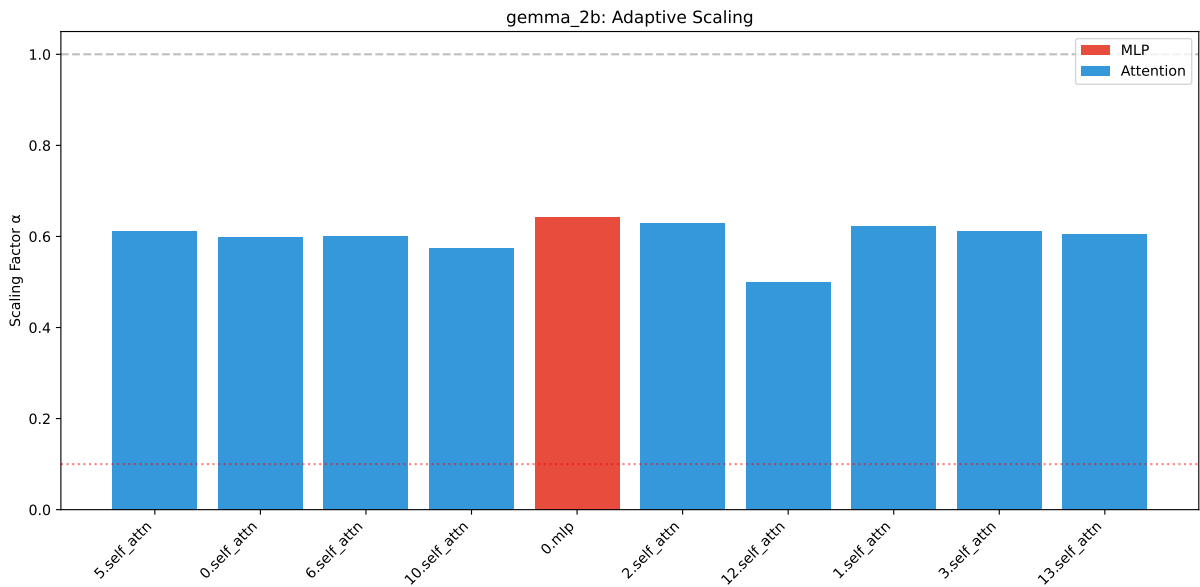


Figure 5: Adaptive scaling factor for the top-10 layer components for Gemma-2B over the RTP dataset. **Takeaway:** Toxicity is higher in the attentions.

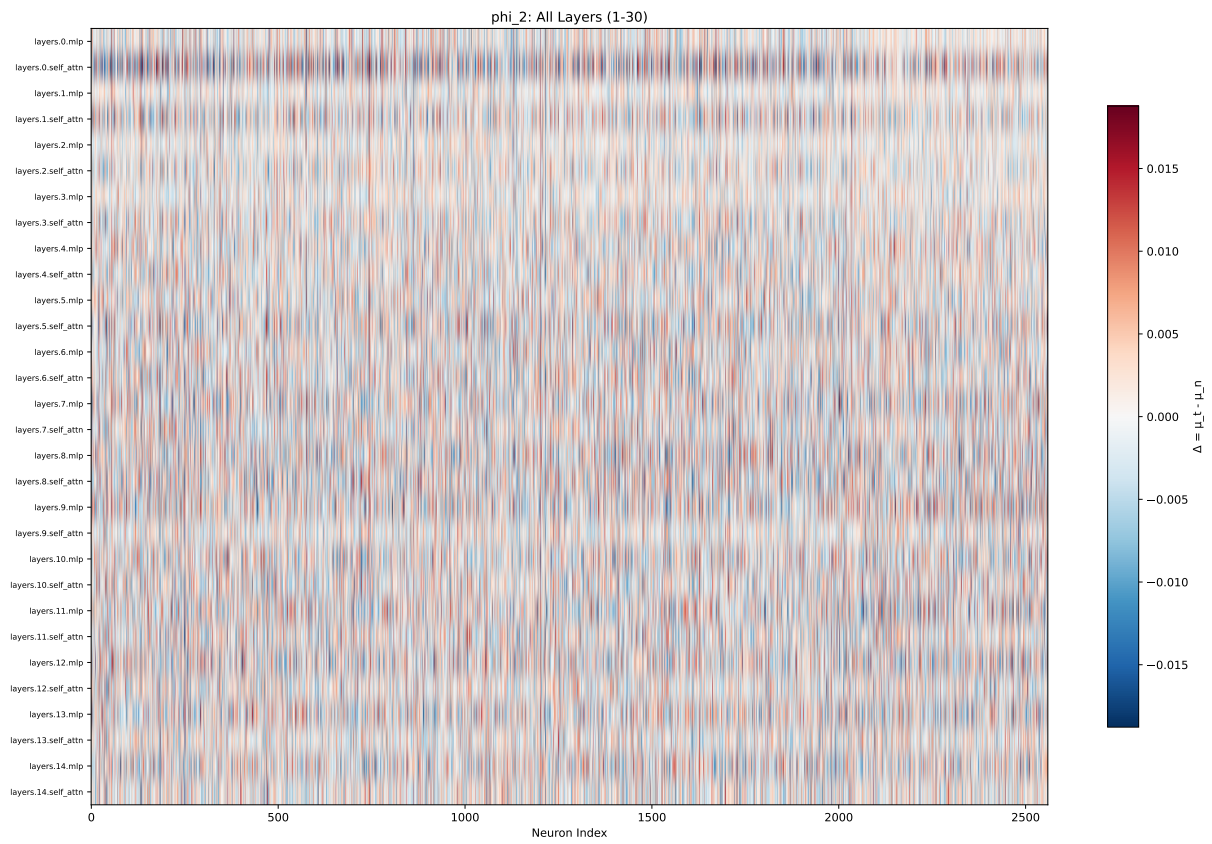


Figure 6: The toxicity detection in attentions and MLPs for Phi-2 over the RTP dataset. **Takeaway:** *The toxicity is highly likely present in both attentions and MLP-layers.*

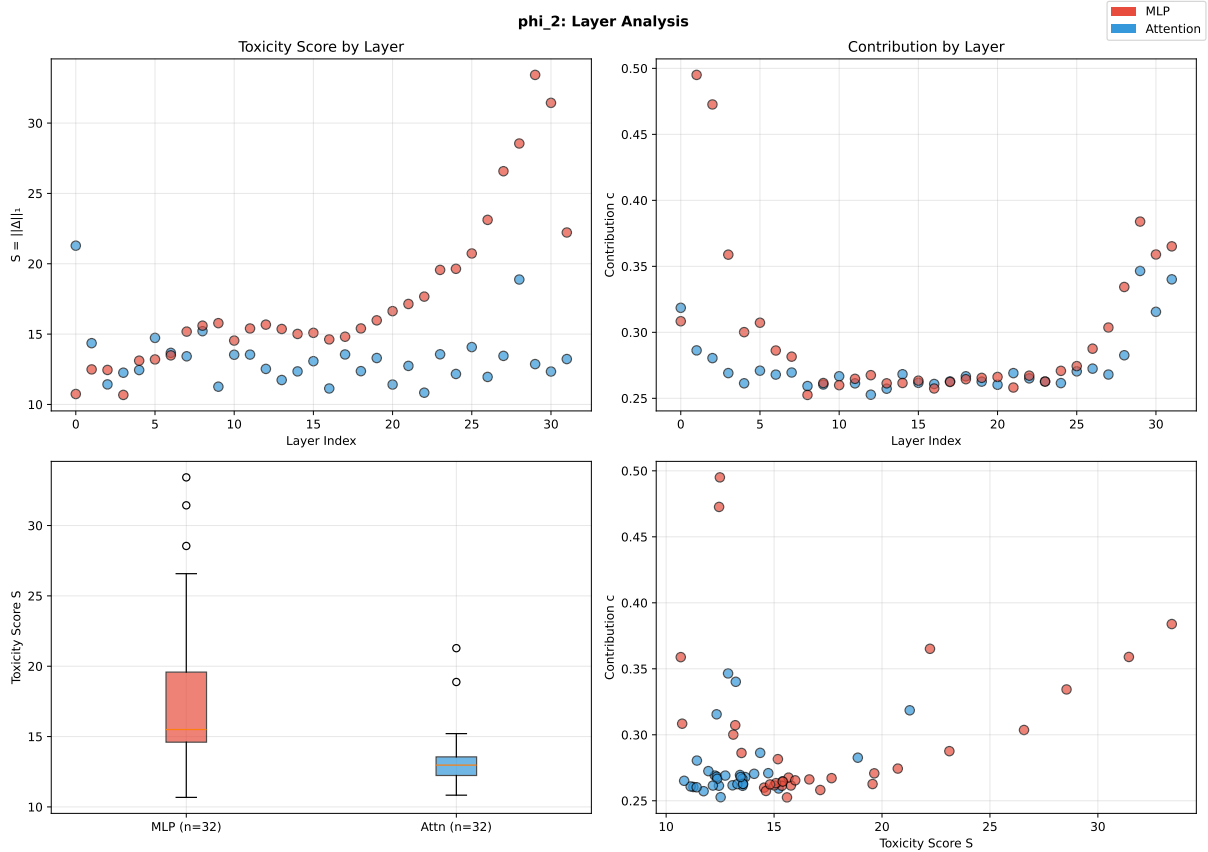


Figure 7: The layer analysis for Phi-2 over the RTP dataset. Here we show the (*top-left*) toxicity scores per layer, (*top-right*) contribution by layers, (*bottom-left*) component vs toxicity score, and (*bottom-right*) toxicity score vs contribution score. **Takeaway:** Toxicity is more observed in the attentions + MLPs of initial layers and MLPs in last layers.

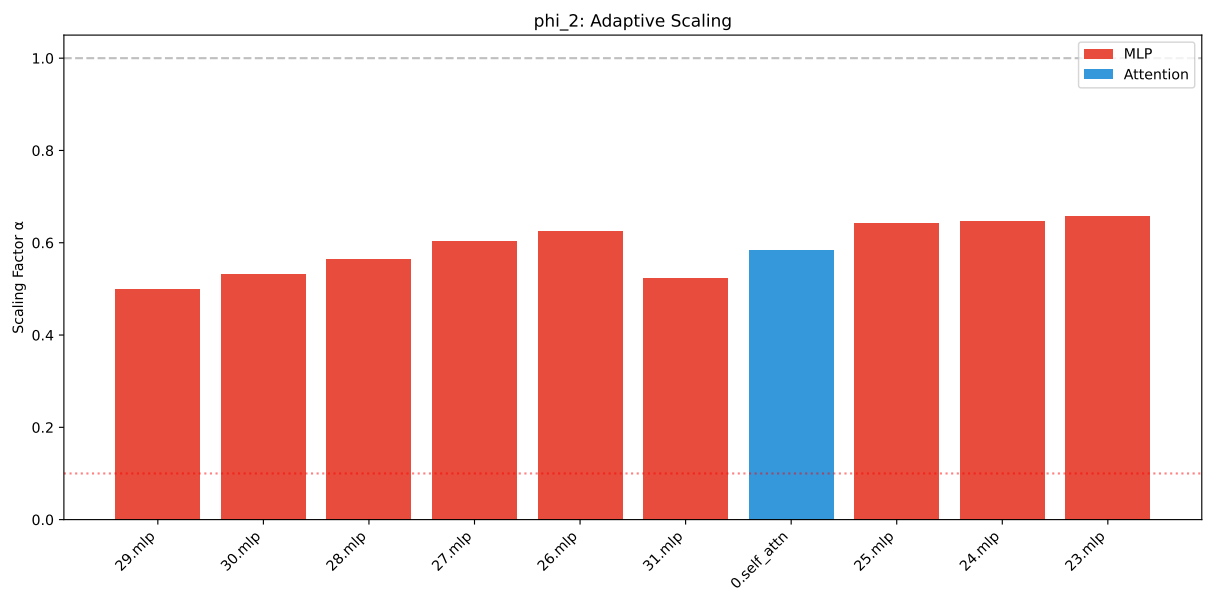


Figure 8: Adaptive scaling factor for the top-10 layer components for Phi-2 over the RTP dataset. **Takeaway:** Toxicity is higher in the MLPs.

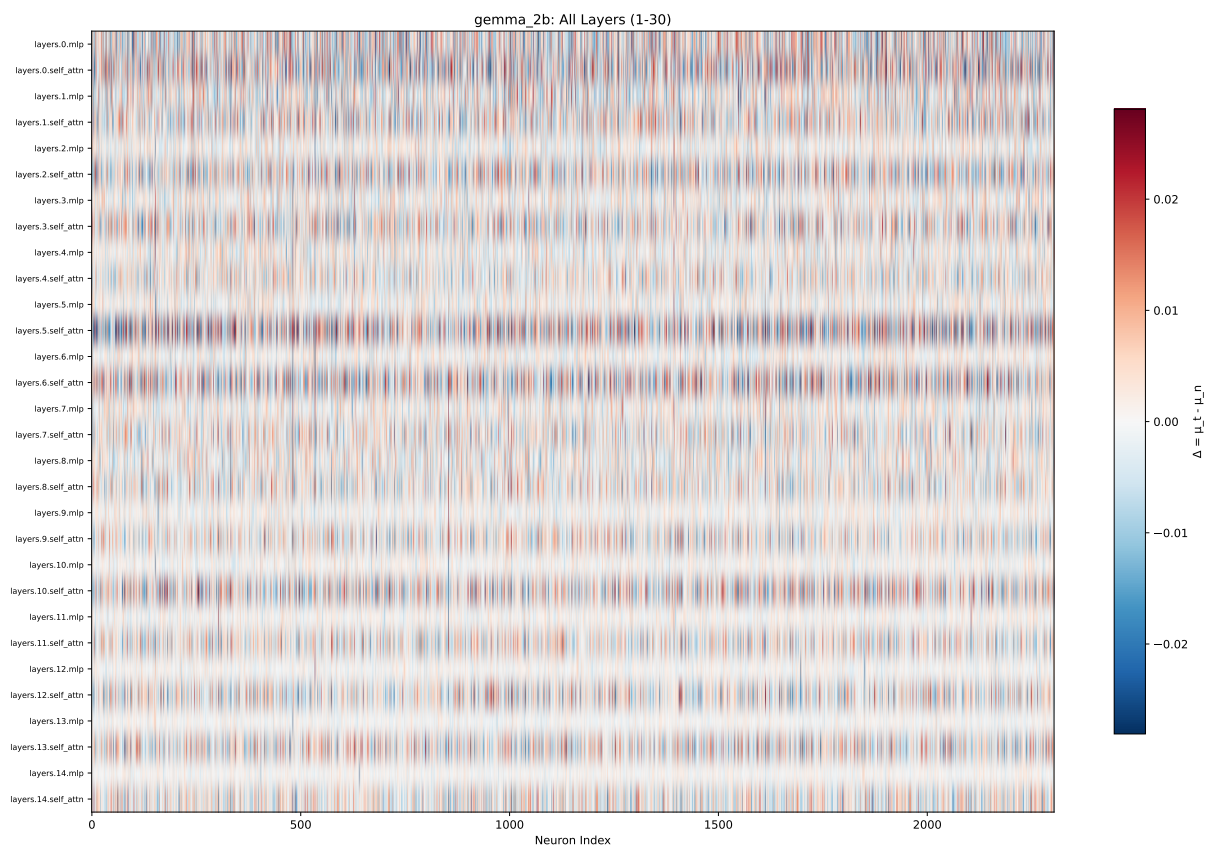


Figure 9: The toxicity detection in attentions and MLPs for Gemma-2B over the RTP dataset. **Takeaway:** *The toxicity is highly likely present in the attentions.*

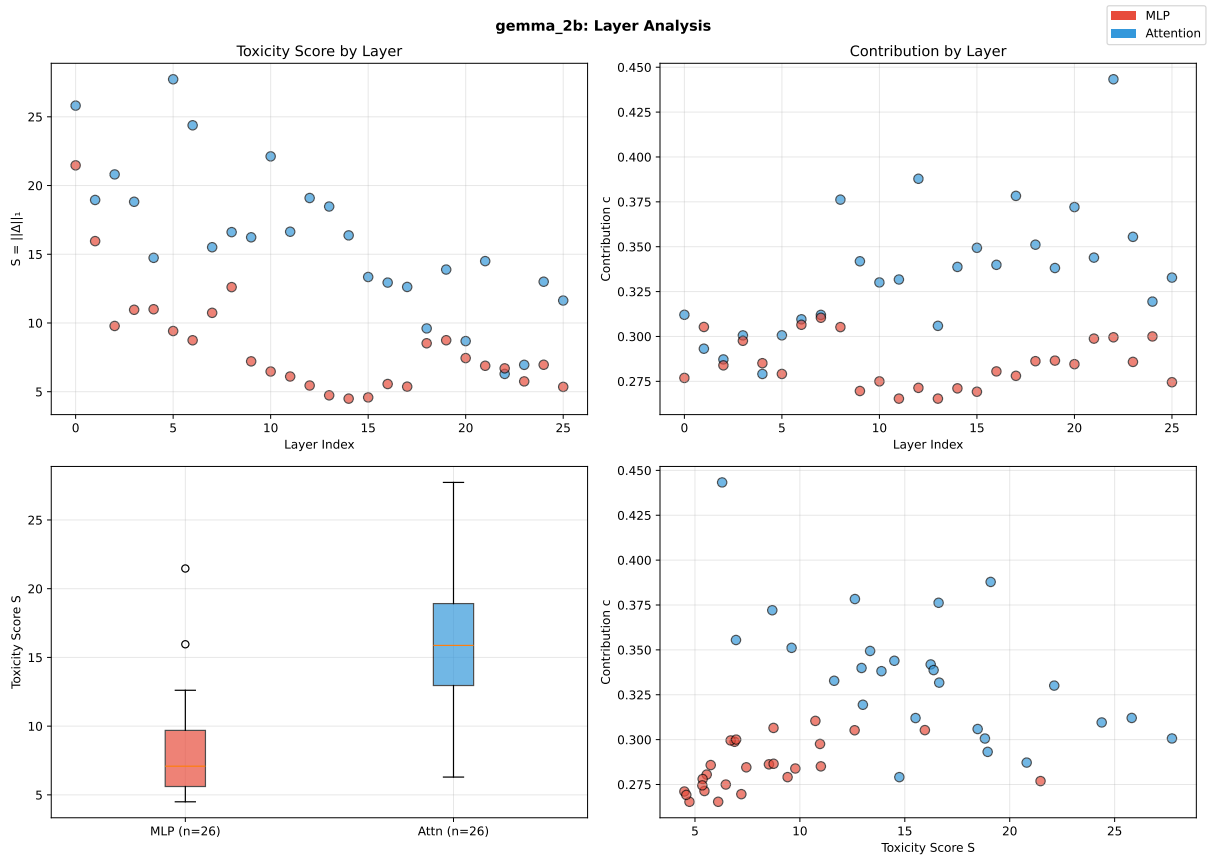


Figure 10: The layer analysis for Gemma-2B over the RTP dataset. Here we show the (*top-left*) toxicity scores per layer, (*top-right*) contribution by layers, (*bottom-left*) component vs toxicity score, and (*bottom-right*) toxicity score vs contribution score. **Takeaway:** Toxicity is more observed in the attentions + MLPs of initial layers and attentions in last layers.

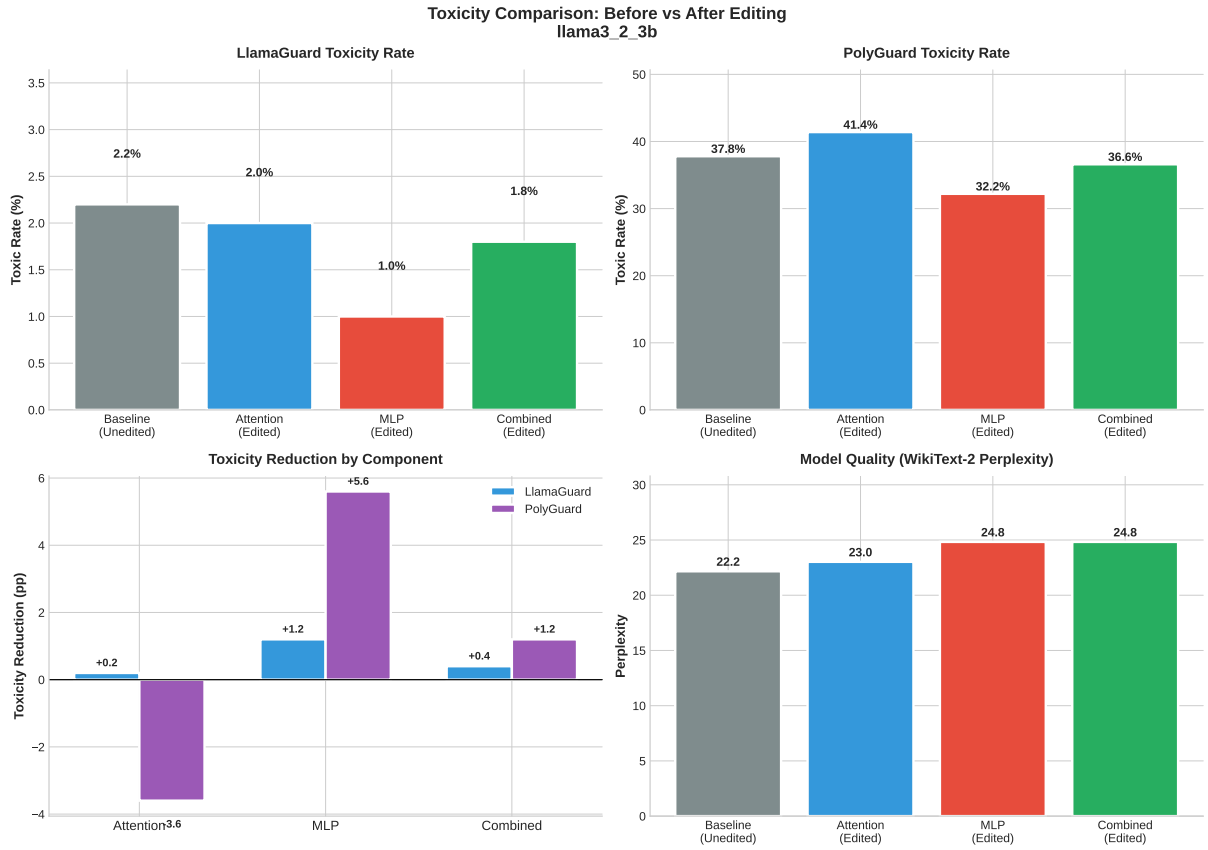


Figure 11: Toxicity reduction and perplexity analysis in attentions, MLPs, and combined for Llama-3.2-3B-Instruct with edit strength of 5 and top 5 layers.

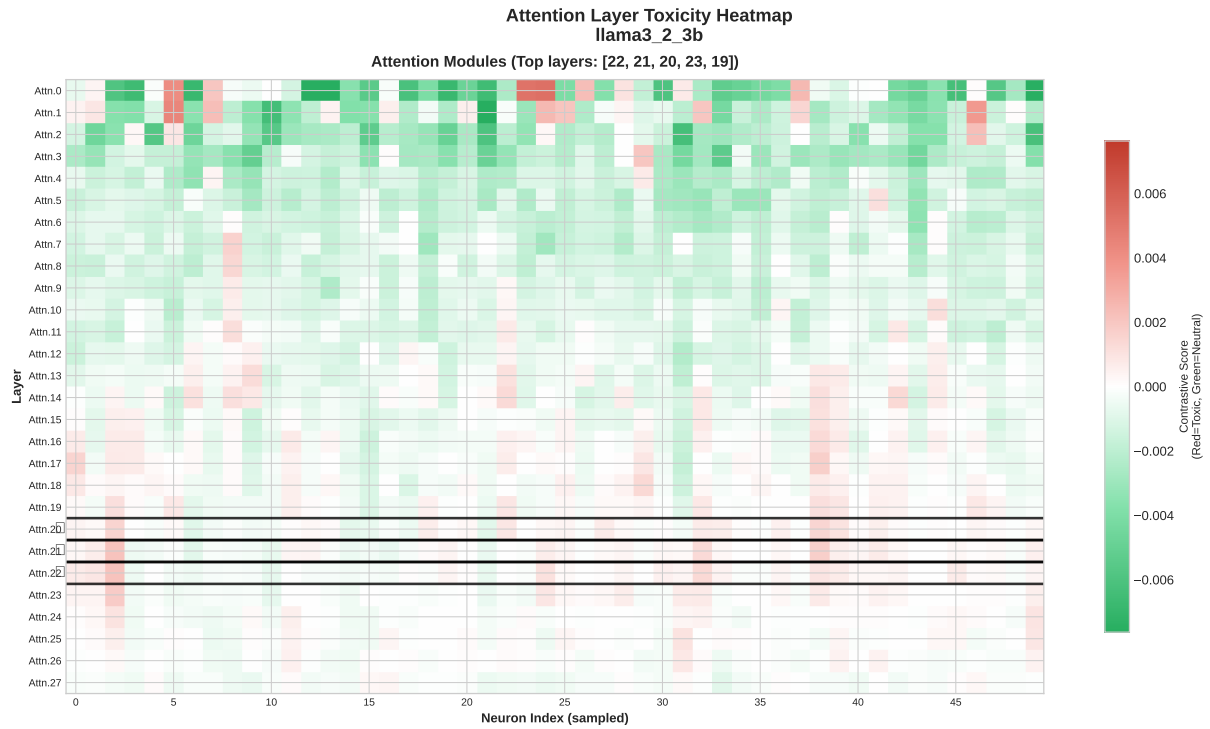


Figure 12: Attention-layers heatmap for Llama-3.2-3B-Instruct with edit strength of 5 and top 5 layers.

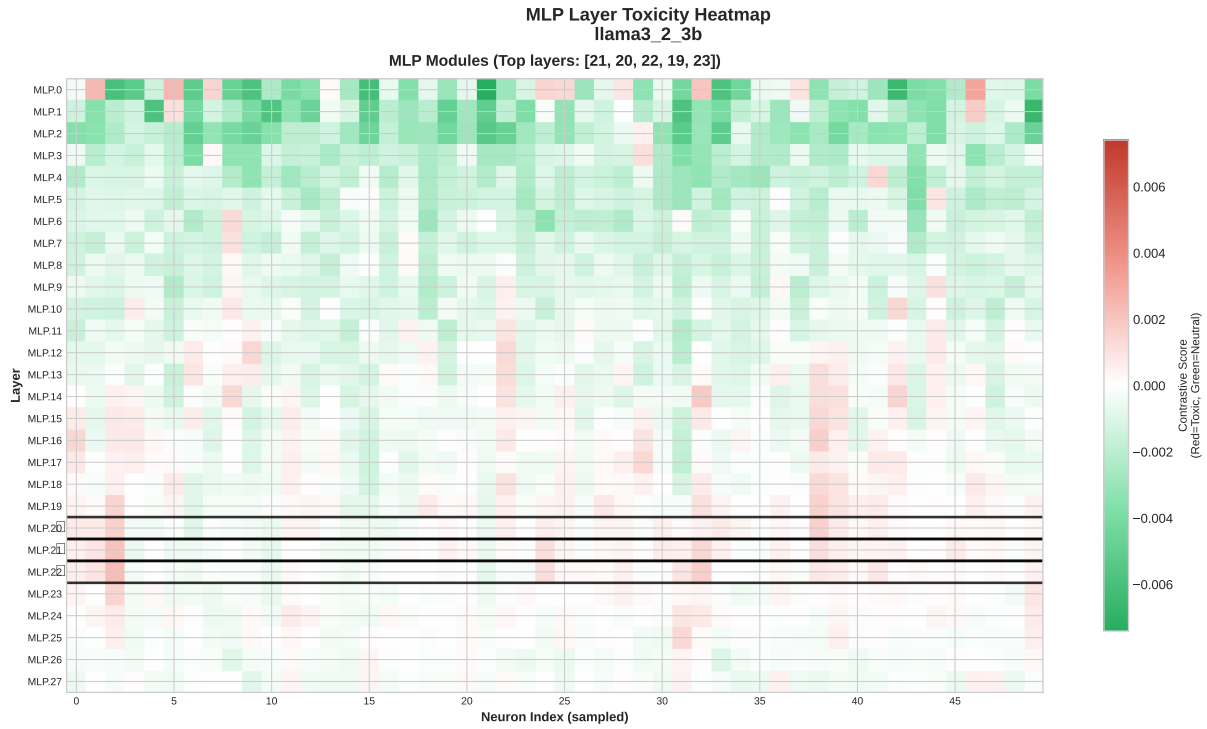


Figure 13: MLP-layers heatmap for Llama-3.2-3B-Instruct with edit strength of 5 and top 5 layers.

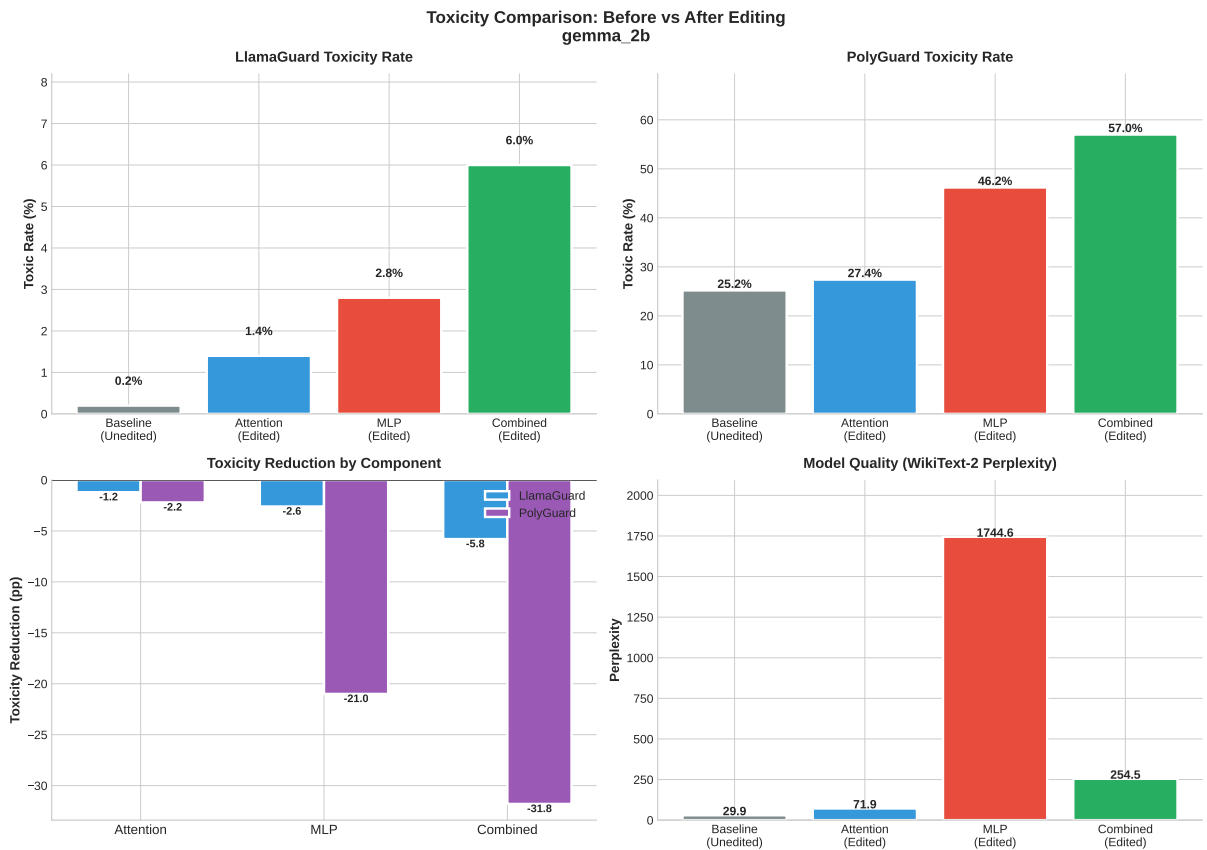


Figure 14: Toxicity reduction and perplexity analysis in attentions, MLPs, and combined for gemma-2-2b-it with edit strength of 20 and top 10 layers.

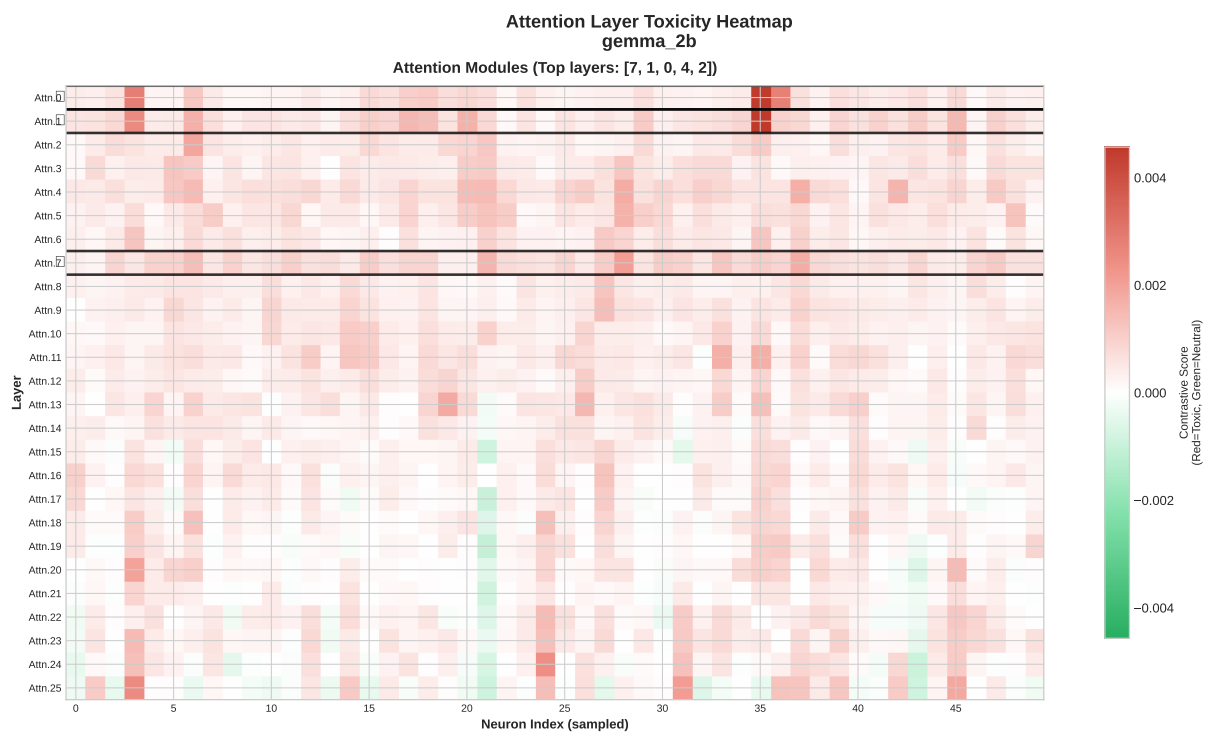


Figure 15: Attention-layers heatmap for gemma-2-2b-it with edit strength of 20 and top 10 layers.

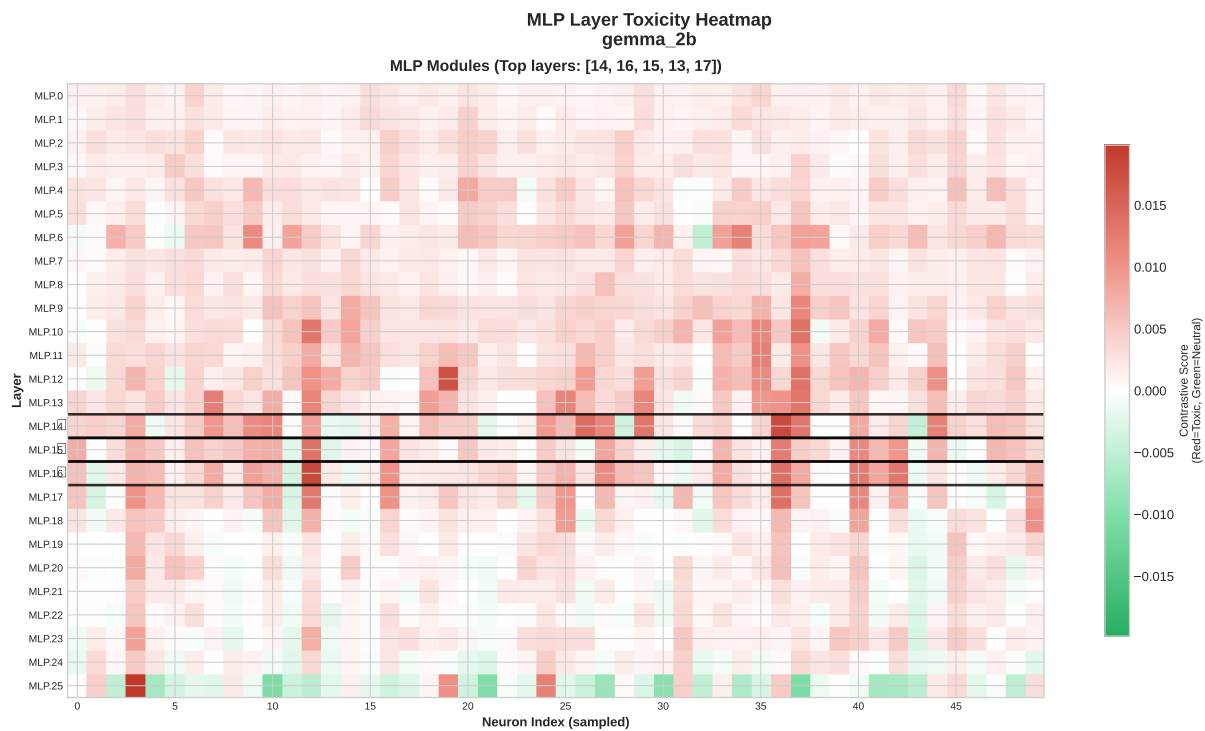


Figure 16: MLP-layers heatmap for gemma-2-2b-it with edit strength of 20 and top 10 layers.

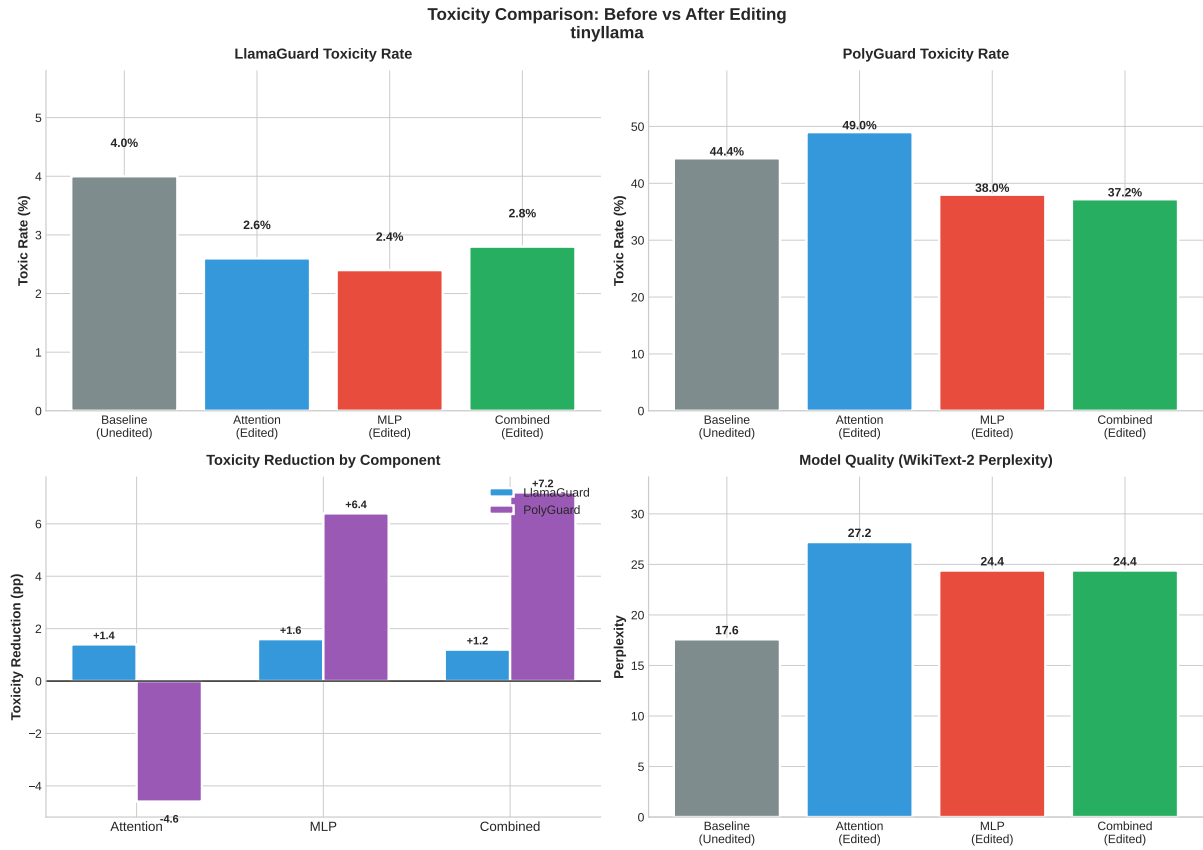


Figure 17: Toxicity reduction and perplexity analysis in attentions, MLPs, and combined for tinyllama with edit strength of 5 and top 10 layers.

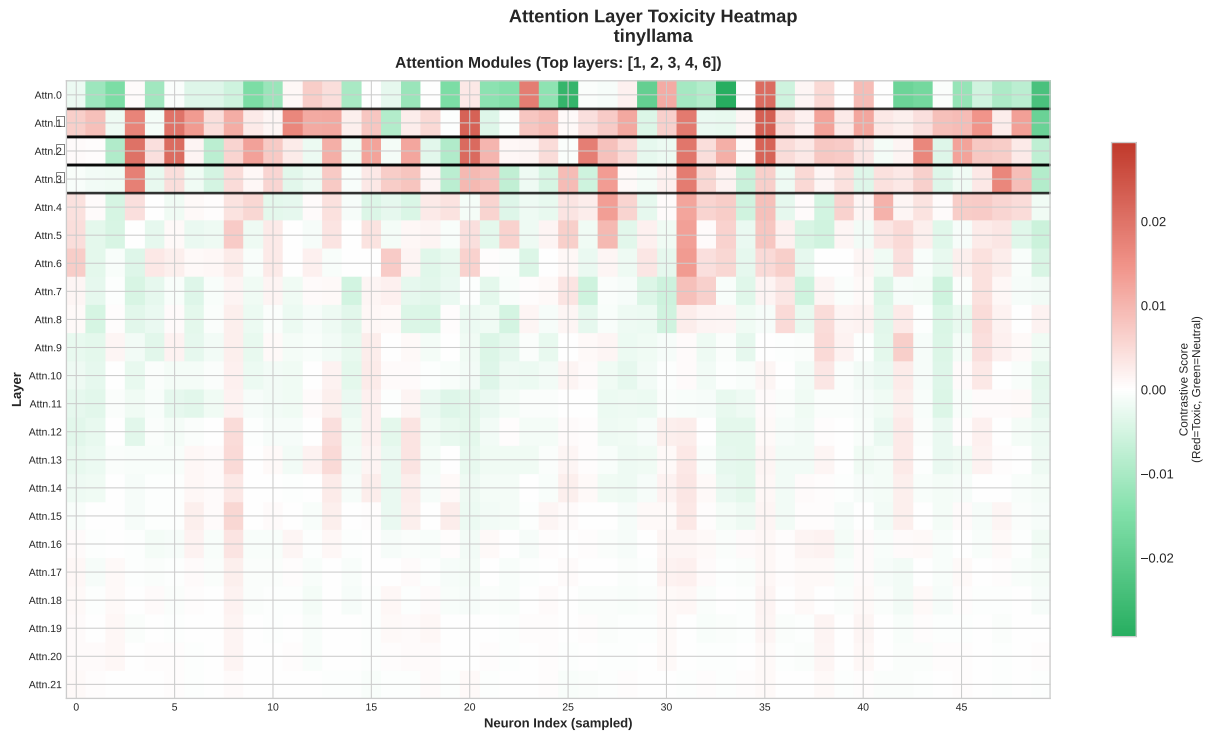


Figure 18: Attention-layers heatmap for tinyllama with edit strength of 5 and top 10 layers.

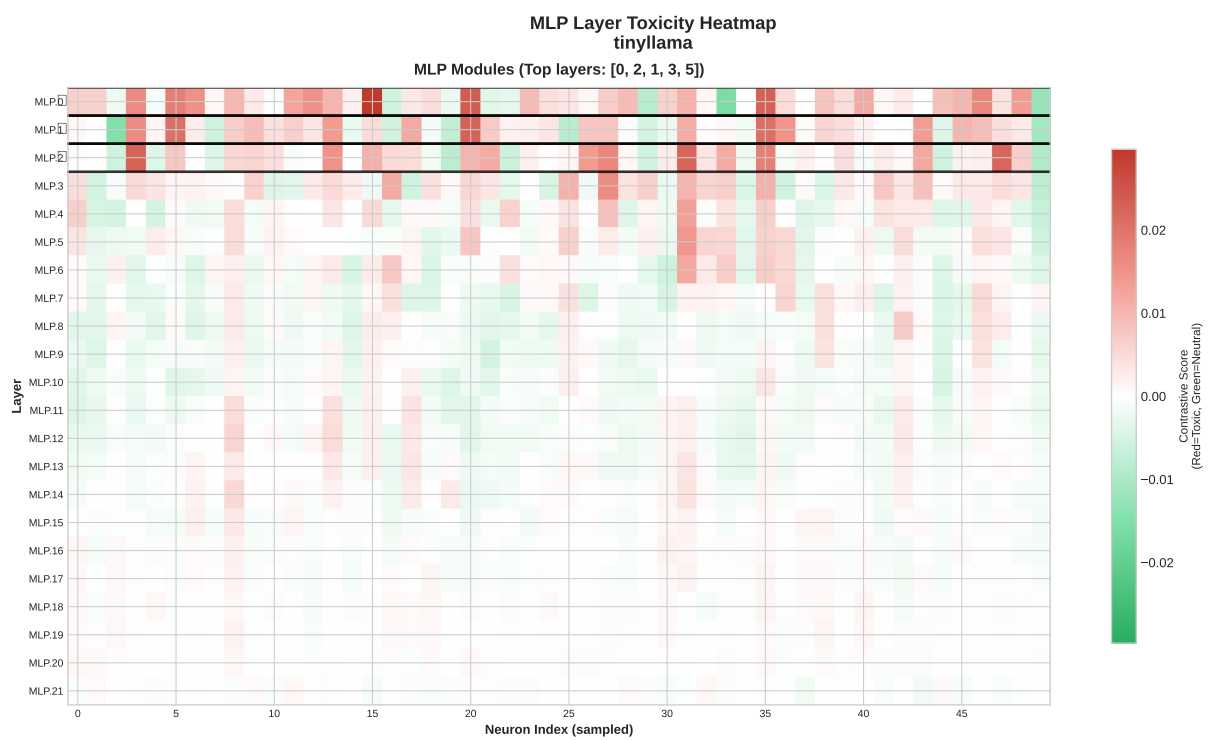


Figure 19: MLP-layers heatmap for tinyllama with edit strength of 5 and top 10 layers.